Version of Record: https://www.sciencedirect.com/science/article/pii/S002192582301880X
Manuscript_6796711f1ef6929584b9f30dbf575c4b

Mistranslation of the genetic code by a new family of bacterial transfer RNAs

Dominik B. Schuntermann[a, b], Jonathan T. Fischer[a], Jonmatthew Bile[a], Sarah A. Gaier[a], Brett A. Shelley[f], Aya Awawdeh[a], Martina Jahn[b], Kyle S. Hoffman[c], Eric Westhof[d], Dieter Söll[a,e,*], Christopher R. Clarke[f], and Oscar Vargas-Rodriguez[a,*,†]

[a] Department of Molecular Biophysics and Biochemistry, Yale University, New Haven, CT 06511, USA
[b] Department of Microbiology, Technical University of Braunschweig, Braunschweig, Germany
[c] Bioinformatics Solutions Inc., Waterloo, ON N2L 6J2, Canada
[d] Université de Strasbourg, Institut de biologie moléculaire et cellulaire du CNRS, 67084 Strasbourg, France
[e] Department of Chemistry, Yale University, New Haven, CT 06511, USA
[f] Genetic Improvement for Fruits and Vegetables Lab, Beltsville Agricultural Research Center, Agricultural Research Service, USDA, Beltsville, MD 20705, USA

[*] To whom correspondence may be addressed: Oscar Vargas-Rodriguez, oscar.vargas@yale.edu; Dieter Söll, dieter.soll@yale.edu.

Present address:
[†] Department of Molecular Biology and Biophysics, University of Connecticut Health Center, Farmington, CT 06030, USA

Running title: Bacterial tRNAs mistranslate the genetic code

Keywords: tRNA, aminoacyl-tRNA synthetase, genetic code, translation, mistranslation, protein synthesis, Streptomyces.

Abbreviations:
tRNA, transfer RNA
aaRS, aminoacyl-tRNA synthetase
ProRS, prolyl-tRNA synthetase
GFP, green fluorescent protein
IPTG, isopropyl-D-thiogalactopyranoside
SDS-PAGE, sodium dodecyl sulfate polyacrylamide gel electrophoresis
BLASTN, basic local alignment search tool

Abstract
The correct coupling of amino acids with transfer RNAs (tRNAs) is vital for translating genetic information into functional proteins. Errors during this process lead to mistranslation, where a codon is translated using the wrong amino acid. While unregulated and prolonged mistranslation is often toxic, growing evidence suggests that organisms, from bacteria to humans, can induce and use mistranslation as a mechanism to overcome unfavorable environmental conditions. Most known cases of mistranslation are caused by translation factors with poor substrate specificity or when substrate discrimination is sensitive to molecular changes such as mutations or post-translational modifications. Here we report two novel families of tRNAs, encoded by bacteria from the *Streptomyces* and *Kitasatospora* genera, that adopted dual identities by integrating the anticodons AUU (for Asn) or AGU (for Thr) into the structure of a distinct proline tRNA. These tRNAs are typically encoded next to a full-length or truncated version of a distinct isoform of bacterial-type prolyl-tRNA synthetase. Using two protein reporters, we showed that these tRNAs translate asparagine and threonine codons with proline. Moreover, when expressed in *Escherichia coli*, the tRNAs cause varying growth defects due to global Asn-to-Pro and Thr-to-Pro mutations. Yet, proteome-wide substitutions of Asn with Pro induced by tRNA expression increased cell tolerance to the antibiotic carbenicillin, indicating that Pro mistranslation can be beneficial under certain conditions. Collectively, our results significantly expand the catalog of organisms known to possess dedicated mistranslation machinery and support the concept that mistranslation is a mechanism for cellular resiliency against environmental stress.

Introduction

Mistranslation of the genetic code, wherein a codon is decoded with the wrong amino acid, is inherent to organisms from all domains of life. In basic cellular conditions, mistranslation is estimated to occur once every 10^3-10^4 translated codons, although environmental and metabolic factors can increase this rate (1-6). Elevated and uncontrolled mistranslation can cause irreparable damage (6-12). However, in recent years, our understanding of mistranslation has been transformed by the discoveries of cellular conditions in which mistranslation is used as a mechanism to overcome unfavorable circumstances. For instance, human cancer cells can withstand immune response challenges by translating Trp codons as Tyr (13). Similarly, global mistranslation with Met can protect mammalian and bacterial cells against oxidative stress (14, 15), while the opportunistic human pathogen *Candida albicans* mistranslates Leu codons with Ser as a mechanism to escape the host's immune response (16-19). Several other examples of mistranslation as a mechanism of cellular resiliency and survival have been described (20-29).

Aminoacyl-tRNA synthetases (aaRSs) and ribosomes are the primary sources of mistranslation. aaRSs catalyze the ligation of amino acids to tRNAs to form the aminoacyl-tRNAs, the substrates for ribosomal protein synthesis. Ribosomes and aaRSs are inherently error-prone, and their specificities are also susceptible to molecular changes (e.g., mutations or modification). Consequently, most reported cases of mistranslation are caused by the ligation of amino acids to the wrong tRNAs or incorrect pairing of aminoacyl-tRNAs with mRNA codons on the ribosomes (27, 30). However, in a few cases, dedicated mistranslation factors exist. For example, *C. albicans* encodes a unique tRNA with a dual identity. As a result, this tRNA is acylated with either Leu or Ser by the corresponding aaRSs, leading to the translation of CUG codons as either Ser or Leu (16-18).

We recently discovered a unique family of proline tRNAs in a group of *Streptomyces* bacteria that includes agriculturally important plant pathogens (31). This peculiar $tRNA^{Pro}$ has adopted a dual identity by replacing its proline anticodon GGG with an AGC alanine anticodon (Fig. 1). To indicate its $tRNA^{Pro}$ structure and alanine anticodon; this tRNA family was named $tRNA^{ProA}$. $tRNA^{ProA}$ is encoded with a distinct isoform of bacterial-type ProRS (called ProRSx), which appears to have co-evolved with $tRNA^{ProA}$. When expressed recombinantly in *E. coli*, $tRNA^{ProA}$ mistranslates Ala codons with Pro, suggesting that organisms encoding $tRNA^{ProA}$ can deliberately mistranslate their genetic code (31). $tRNA^{ProA}$ is one of the first examples of a bacterial tRNA that evolved to mistranslate a sense codon.

In the present work, we report two new families of non-canonical tRNAs encoded by Gram-positive bacteria from the *Streptomyces* and *Kitasatospora* genera. Both tRNA families have a $tRNA^{ProA}$-like structure but have adopted either an AUU anticodon (Asn) or an AGU anticodon (Thr) (Fig. 1). Like $tRNA^{ProA}$, the tRNAs are encoded next to a putative ProRSx gene, although a truncated version of ProRSx is found in some cases. We show that these novel tRNAs mistranslate their corresponding codons with Pro, leading to proteome-wide Asn-to-Pro and Thr-to-Pro changes. Pro mistranslation caused varying degrees of growth defects in *E. coli* based on the nature of the mistranslated codon. Despite the harmful impact on cell fitness, we observed that the expression of the tRNA mistranslators increased the resistance of *E. coli* to the antibiotic carbenicillin.

Results

Identification of tRNAs with dual identity

We previously determined that $tRNA^{ProA}$ genes are annotated as alanine tRNAs ($tRNA^{Ala}$) in genomic databases due to automated annotation algorithms' reliance on the anticodon sequence to establish the identity of tRNA genes. Consequently, the AGC anticodon of $tRNA^{ProA}$ causes its annotation as $tRNA^{Ala}$, which hindered a complete assessment of the phylogenetic distribution of $tRNA^{ProA}$ genes. To circumvent this, we performed searches based on sequence homology using the *S. turgidiscabies* $tRNA^{ProA}$ as a query. The search identified 18 new genomes containing a region with a predicted tRNA gene and high homology to $tRNA^{ProA}$. While all the identified tRNA genes contained the signature C1:G72 base pair of $tRNA^{ProA}$ and $tRNA^{Pro}$, only six tRNAs had the AGC anticodon of $tRNA^{ProA}$. Surprisingly, the remaining tRNA genes had either an Asn AUU (1 genome) or a Thr AGU (11 genomes) anticodon (Figs. 1 and S1). These genes are annotated as $tRNA^{Asn}$ and $tRNA^{Thr}$ according to their anticodon sequence. However, like $tRNA^{ProA}$, the tRNAs lack the known key elements for aminoacylation by their cognate aaRS (32), suggesting that they are not paired with the amino acids corresponding to their anticodon. Given the Asn or Thr anticodon combination with the Pro identity element, we named the tRNAs, $tRNA^{ProN}$, and $tRNA^{ProT}$ (Fig. 1). Using the newly discovered $tRNA^{ProN}$ and $tRNA^{ProT}$ sequences as queries, we performed new searches that unearthed 21 additional organisms with $tRNA^{ProA}$ (7), $tRNA^{ProN}$ (1), and $tRNA^{ProT}$ (13). Notably, $tRNA^{ProN}$ and $tRNA^{ProT}$ contain the same unusual and unique structural features of $tRNA^{ProA}$ (33), including adenosine at positions 33 (A33) and 34 (A34), an A15:A48 tertiary pair, and a G21 (although several $tRNA^{ProT}$ species contain A21) (Figs. 1 and S1). Because of the conservation of these elements, $tRNA^{ProA}$, $tRNA^{ProN}$, and $tRNA^{ProT}$ appear to have originated from a common ancestral tRNA and belong to a single class of non-canonical tRNAs, which we named the $tRNA^{ProX}$ family.

A unique ProRS isoform encoded with $tRNA^{ProX}$

The discovery of $tRNA^{ProN}$ and $tRNA^{ProT}$ prompted us to examine their genomic context. We previously showed that $tRNA^{ProA}$ is encoded next to a *proSx* gene encoding ProRSx, a distinct form of bacterial prolyl-tRNA synthetase (ProRS) (31). Consistent with this observation, we found that every newly identified $tRNA^{ProA}$ gene is flanked by a *proSx* gene except for *Streptomyces vinaceus*, which lacks this gene (Figs. 2A and S2). Furthermore, almost half of the bacteria that encode $tRNA^{ProT}$ also possess a *proSx* gene (Figs. 2A and S2). However, in the other half of organisms with $tRNA^{ProT}$ and the two encoding $tRNA^{ProN}$, a truncated *proSx* gene encoding roughly 200 residues is found (Figs 2A and S2). Sequence alignments showed that the remaining section of the gene matches the C-terminal region of the ProRSx protein, which comprises the tRNA anticodon binding domain (ABD) (Figs. 2A and S3). A phylogenetic analysis of the ProRS enzymes revealed two distinct clades for ProRSx, indicating that ProRSx emerged from the bacterial-type ProRS and continued to evolve divergently (Fig. 2B). The divergence of the ProRSx enzyme family appears to be related to the identity of their accompanying $tRNA^{ProX}$ gene as ProRSx located with the $tRNA^{ProN}$ and $tRNA^{ProT}$ cluster separately from ProRSx sequences encoded with $tRNA^{ProA}$ (Fig. 2B). This suggests that ProRSx has co-evolved with the corresponding tRNAs to adapt to changes in the anticodon. Thus, we surmise that the last base of the anticodon may have been the evolutionary driving force since $tRNA^{ProN}$ and $tRNA^{ProT}$ share U36 and $tRNA^{ProA}$ contains C36. A multiple sequence alignment guided by the bacterial ProRS-$tRNA^{Pro}$ complex showed that the residues predicted to interact with N36 vary between the two ProRSx subfamilies (Fig. S3) (31).

Phylogenetic distribution and evolution of ProRSx and $tRNA^{ProX}$

The 46 organisms now known to encode ProRSx and $tRNA^{ProX}$ are found in bacteria from the *Actinomycetes* class, primarily in *Streptomyces* species and a few *Kitasatospora* species (Table S1 and Fig. S1). These organisms represent a small subset of the more than 3000 *Streptomycetaceae* genomes that are publicly available. Notably, these genes are encoded in four of the more than twelve species known to cause plant diseases, including strains of *Streptomyces ipomoeae* (34), *Streptomyces turgidiscabies, Streptomyces reticuliscabiei* (35) (same genomospecies), *Streptomyces griseiscabiei* (36), and *Streptomyces caniscabiei* (37, 38). However, in several cases, ProRSx/$tRNA^{ProX}$ is only present in one of the several available strains of these pathogens, suggesting either a recent acquisition or ancestral loss with maintenance in only one known lineage.

To better contextualize the phylogenetic distribution and evolution of ProRSx and $tRNA^{ProX}$, we constructed a phylogenetic tree to represent the relationship between select strains of *Streptomyces*, *Kitasatospora*, and *Streptacidiphilus* using multilocus sequence analysis (39). In addition to the 46 genomes encoding ProRSx and $tRNA^{ProX}$, we included 38 strains to represent the large diversity of *Streptomyces* (39), the three major clades of *Kitasatospora* (40), and *Streptacidiphilus* (41). While no available genomes of *Streptacidiphilus* contain ProRSx, the genus was included because it is sister to the *Kitasatospora* genus (40). Whether the ancestor of *Streptacidiphilus* lost ProRSx or if ancestral lineages of *Kitasatospora* and *Streptomyces* independently gained ProRSx remains unknown. The analysis revealed that ProRSx and all three $tRNA^{ProX}$ families are distributed sporadically within the *Streptomyces* genus, while ProRSx and $tRNA^{ProT}$ are present in two of the three defined clades of *Kitasatospora* (Fig. 3). Based on its presence across multiple genera, we hypothesize that $tRNA^{ProT}$ is the most ancestral $tRNA^{ProX}$, even though $tRNA^{ProA}$ is more prevalent in *Streptomyces*. Moreover, the presence of $tRNA^{ProN}$ in only two closely related *Streptomyces* strains indicates that it emerged more recently.

Interestingly, *Streptomyces odonnellii* clustered with other strains that encode the $tRNA^{ProT}$, suggesting that the duplication of the $tRNA^{ProT}$ gene is a recent event. Whether the polyphyletic distribution of ProRSx and the three members of $tRNA^{ProX}$ results from horizontal gene transfer of the genomic locus or ancestral loss of the genes in most lineages of *Streptomycetaceae* is unknown.

$tRNA^{ProT}$ translates Thr codons as Pro

To investigate whether $tRNA^{ProT}$ mistranslates Thr codons with Pro, we adapted our previously developed dual fluorescence reporter consisting of a fusion of superfolder green fluorescent protein (sfGFP) and the red fluorescent mCherry in *E. coli* (Fig. 4A) (31). The reporter is based on the critical role of the residue Thr65 in forming the sfGFP fluorophore. Pro at this position prevents proper fluorophore formation, causing a complete loss of the sfGFP fluorescence (31, 42). mCherry is used to normalize sfGFP expression. Thus, we expected that cells expressing $tRNA^{ProT}$ and sfGFP-mCherry would display a lower sfGFP/mCherry emission ratio than cells without $tRNA^{ProT}$ (Fig. 4B). Indeed, we observed a ~7-fold reduction in sfGFP/mCherry fluorescence emission in *E. coli* cells expressing $tRNA^{ProT}$ (Fig. 4C), indicating that $tRNA^{ProT}$ can incorporate Pro in response to Thr codons. Interestingly, the co-expression of $tRNA^{ProT}$ with its cognate ProRSx only marginally increased sfGFP/mCherry fluorescence, suggesting that endogenous *E. coli* ProRS aminoacylates $tRNA^{ProT}$.

Mistranslation of Asn codons by $tRNA^{ProN}$

We next sought to test whether $tRNA^{ProN}$ can mistranslate Asn codons with Pro. Because Asn at position 65 of sfGFP also impairs chromophore formation (42), this reporter was unsuitable for studying Asn-to-Pro mistranslation. Instead, we adopted a gain-of-function reporter based on β-lactamase activity. We previously reported that a Pro residue at position 65 of β-lactamase is essential for its catalytic activity. Consequently, cells encoding the P65A β-lactamase mutant are sensitive to the antibiotics ampicillin and carbenicillin (31). To evaluate whether Asn has a similar effect, we mutated the Pro65 codon to AAU (Asn) in β-lactamase and compared its activity to wild-type (wt) β-lactamase in *E. coli*. We observed that cells expressing the P65N β-lactamase did not grow in media containing ampicillin, whereas cells expressing the wt enzyme displayed robust growth (Fig. 5A). This result further supports that Pro65 is essential for β-lactamase and enabled us to repurpose its activity to investigate Asn-to-Pro mistranslation. We expected that mistranslation of Asn at position 65 with Pro would yield a sufficient fraction of active β-lactamase that should increase antibiotic tolerance (Fig. 5B). Thus, we expressed P65N β-lactamase in *E. coli* in the absence or presence of $tRNA^{ProN}$ and tested cell growth on agar plates containing varying concentrations of carbenicillin. Because $tRNA^{ProN}$ is found next to a truncated *proSx* gene, we tested the tRNA alone. As expected, *E. coli* expressing the P65N β-lactamase variant alone showed significantly impaired growth in the presence of the antibiotic (Fig. 5C). In contrast, cells expressing $tRNA^{ProN}$ displayed a substantial tolerance to carbenicillin, even at the highest concentration tested (Fig. 5C).

To confirm the incorporation of Pro in response to Asn codons, we used an sfGFP reporter with an N-terminal extension previously developed to facilitate the detection of mistranslation events using liquid chromatography-tandem mass spectrometry (LC-MS/MS) (43). The 26-residue extension contains a hydrophobic peptide sequence that provides reliable ionization. The sfGFP reporter was recombinantly expressed and purified from *E.*

coli cells with and without $tRNA^{ProN}$ co-expression and analyzed by LC-MS/MS. Interestingly, while no Pro misincorporation was identified at the targeted position of the N-terminal extension, Asn-to-Pro mistranslation was detected at three different positions within sfGFP corresponding to N115, N144, and N185 (Fig. S4). These substitutions were not observed in the sfGFP purified in the absence of $tRNA^{ProN}$. These results demonstrate that $tRNA^{ProN}$ can mistranslate Asn codons with Pro.

Expression of $tRNA^{ProX}$ is toxic in E. coli

To investigate the effect of mistranslation on cell fitness, we constitutively expressed *S. turgidiscabies* $tRNA^{ProA}$, *Streptomyces* sp. OK228 $tRNA^{ProN}$, and *Kitasatospora setae* $tRNA^{ProT}$ in *E. coli* with or without their cognate ProRSx, except for $tRNA^{ProN}$ which is only encoded with a truncated ProRSx (Figs. 2A and S2). Consequently, we chose *K. setae* ProRSx (*Ks*ProRSx) for co-expression with $tRNA^{ProN}$, given the phylogenetic relationship between *Ks*ProRSx and the truncated *Streptomyces* sp. OK228 ProRSx (Fig. 2B). Notably, individual expression of the three tRNAs was toxic in *E. coli* cells, albeit with different degrees of severity (Fig. 6). $tRNA^{ProA}$ caused a minor growth defect, whereas $tRNA^{ProN}$ robustly impaired growth. In contrast, $tRNA^{ProT}$ expression almost completely inhibited cell growth**.** Interestingly, cell cultures expressing $tRNA^{ProT}$ formed white precipitated clumps, suggesting that Thr-to-Pro mistranslation causes cell wall disruption and lysis (Fig. 6C). Lastly, co-expression of the cognate *proSx* genes slightly augmented the growth defect of $tRNA^{ProT}$ but not of $tRNA^{ProA}$ and $tRNA^{ProN}$. The severity of the growth phenotypes by $tRNA^{ProX}$ was also visible in the colony sizes of cells expressing the tRNAs after plasmid transformation. (Fig. 6C). These data suggest that the constitutive mistranslation of Ala, Asn, and Thr codons with Pro is toxic for *E. coli*.

Aminoacylation of $tRNA^{ProX}$ by E. coli ProRS

An intriguing observation from our results is that expression of ProRSx was not necessary for $tRNA^{ProN}$- and $tRNA^{ProT}$-mediated mistranslation in *E. coli* (Figs. 4 and 6), suggesting that endogenous *E. coli* ProRS aminoacylates both tRNAs. Efficient aminoacylation by *E. coli* ProRS relies on the recognition of conserved bases in the $tRNA^{Pro}$ anticodon (G35 and G36) and acceptor stem (A73 and G72) (44, 45). All members of the $tRNA^{ProX}$ family have A73 and G72 but contain either U or C at position 36 (Figs. 1 and S1). Moreover, $tRNA^{ProT}$ and $tRNA^{ProA}$ have a G35, whereas $tRNA^{ProN}$ has a U35. We posited that the presence of these elements in $tRNA^{ProX}$ might enable their recognition and aminoacylation by *E. coli* ProRS. To test this hypothesis, we performed *in vitro* aminoacylation assays using *E. coli* ProRS and *in vitro* tRNA transcripts. The results showed that *E. coli* ProRS has a lower aminoacylation efficiency towards all three $tRNA^{ProX}$ relative to its cognate $tRNA^{Pro}$ substrate (Figs. 7A and S5). However, the enzyme displayed different efficiencies towards each $tRNA^{ProX}$. Although $tRNA^{ProT}$ was aminoacylated almost 4 times less than $tRNA^{Pro}$, it was charged ~3 and 36 times better than $tRNA^{ProN}$ and $tRNA^{ProA}$, respectively. The higher aminoacylation of *E. coli* ProRS for $tRNA^{ProT}$ may be due to the recognition of U36, as *E. coli* ProRS was shown to aminoacylate a G36U $tRNA^{Pro}$ mutant 19-fold more efficiently than a G36C mutant (Fig. 7B) (45). Next, we tested the aminoacylation level of $tRNA^{ProX}$ in *E. coli*. Total RNA was extracted from *E. coli* expressing a $tRNA^{ProX}$ under acidic conditions to retain the amino acid bound to tRNAs. A fraction of each $tRNA^{ProX}$ sample was treated with a basic solution to cleave the amino acid, which allows distinguishing between aminoacylated and deacylated tRNA using specific probes for each tRNA and northern blotting. Total RNA from *E. coli* without $tRNA^{ProX}$ was used as a negative

control. Interestingly, these assays showed that the three tRNAs are mostly aminoacylated *in vivo* (Fig. 7C). While this experiment does not reveal the amino acid attached to the tRNAs, aminoacylation by *E. coli* ProRS is likely possible, given the Pro identity elements of $tRNA^{ProX}$.

Pro mistranslation of Ala and Asn codons benefits E. coli under antibiotic stress

As shown above, mistranslation by $tRNA^{ProN}$ and $tRNA^{ProA}$ negatively affects cell growth under normal growth conditions (Fig. 6). However, mistranslation may offer an adaptive mechanism for survival under specific stress conditions, such as in the presence of antibiotics (28, 46, 47). To assess whether mistranslation by $tRNA^{ProA}$ or $tRNA^{ProN}$ is beneficial, we grew *E. coli* expressing the tRNAs with β-lactamase on LB-agar plates containing different concentrations of carbenicillin (Fig. 8A). We reasoned that if mistranslation offers an advantage, cells expressing the mistranslating tRNA could tolerate higher antibiotic concentrations. Notably, we found that, while mistranslating cells showed a growth defect on plates without carbenicillin, they grew on plates with higher antibiotic concentrations than cells with an empty plasmid (Fig. 8B). Mistranslating cells also showed higher tolerance to ampicillin (Fig. S6). The decreased sensitivity to these β-lactam antibiotics was only observed when β-lactamase was co-expressed with the tRNAs (Fig. S6). These results provide new evidence supporting the positive consequences of mistranslation.

Discussion

Here we described the identification and characterization of $tRNA^{ProN}$ and $tRNA^{ProT}$, a new class of bacterial tRNAs, sparsely present throughout two genera of *Actinomycetota*, that emerged to mistranslate the genetic code. The discovery of $tRNA^{ProN}$ and $tRNA^{ProT}$ adds to the growing number of naturally occurring tRNA mistranslators reported in recent years, including several bacterial and human tRNAs (9, 48-52). The discovery of mistranslating tRNAs has been possible by re-examining sequenced genomes and reclassifying the annotated tRNA genes using a holistic analysis of each tRNA sequence and the predicted secondary structure. This approach allows the recognition of small nuances passed over by automated, high-throughput tRNA search algorithms. With the vast number of sequenced genomes, we predict that more examples of mistranslating tRNAs may be uncovered by carefully reanalyzing tRNA genes detected in these genomes.

The characterization of $tRNA^{ProN}$ and $tRNA^{ProT}$ in *E. coli* showed that the impact of Pro mistranslation on cell fitness depends greatly on the identity of the mistranslated codon. Thr-to-Pro mistranslation was significantly more toxic than Asn-to-Pro mistranslation. In contrast, Ala-to-Pro mistranslation was more tolerated. This difference in toxicity is remarkable because replacing residues with Pro is expected to severely affect protein structure and function (53). However, our results suggest that the substitution of Thr and Asn with Pro is more disruptive to proteins than Ala substitutions with Pro. This may be explained by the expanded catalytic and structural roles of Thr and Asn in proteins relative to the more inert function of Ala. The $tRNA^{ProX}$ aminoacylation efficiency of *E. coli* ProRS may also contribute to the distinct cellular toxicities. The harmful effect of each tRNA correlates with the *in vitro* aminoacylation activity of *E. coli* ProRS. Thus, the ability of *E. coli* ProRS to aminoacylate $tRNA^{ProT}$ more efficiently could result in higher levels of mistranslation relative to the other two tRNAs. $tRNA^{ProT}$ could also influence Pro-$tRNA^{Pro}$ synthesis by competing for ProRS aminoacylation with endogenous $tRNA^{Pro}$. We also considered the possible contribution of codon usage to the differences in toxicity. In *E. coli*, Ala codons represent 9.46% of

predicted codons, whereas Thr and Asn codons comprise 5.38% and 3.92%, respectively (54). The higher Ala codon usage is inversely correlated to the severity of the observed phenotype for mistranslation of Ala codons, thus, reinforcing the notion that proteins can endure Ala-to-Pro substitutions more effectively than Thr-to-Pro and Asn-to-Pro mutations. On the other hand, the mild toxicity of Asn-to-Pro relative to Thr-to-Pro may be due to the lower number of Asn codons. Different patterns of cellular toxicity have also been observed for other forms of mistranslation. Notably, *E. coli* was shown to withstand a variety of mistranslation forms such as Cys and Glu mistranslation at Pro and Gln codons, respectively (55). Recently, Gly-to-Ala mistranslation in human cells was shown to be less harmful than Ser misincorporation at Phe codons (52). In yeast, Ala mistranslation revealed codon-specific growth defects (56). Therefore, it is becoming clear that not all forms of mistranslation are equal and that the nature of mistranslated codons determines the biological impact of mistranslation, while additional factors may contribute to the distinct growth phenotypes. Lastly, the differences in $tRNA^{ProX}$-induced toxicity may provide clues about the phylogenetic distribution and evolution of the $tRNA^{ProX}$ family. $tRNA^{ProA}$, the least toxic of the three $tRNA^{ProX}$, is present in more species relative to $tRNA^{ProT}$ and $tRNA^{ProN}$, and it is always encoded with a full-length ProRSx (except for *S. vinaceus*). Thus, selection may act against the more toxic $tRNA^{ProT}$ and $tRNA^{ProN}$, resulting in the partial deletion or inactivation of ProRSx and a more limited phylogenetic distribution.

The specific mechanism for how Pro mistranslation of Asn and Ala codons increases carbenicillin tolerance in *E. coli* has yet to be elucidated. Interestingly, other forms of mistranslation have also been shown to decrease antibiotic sensitivity. In *E. coli*, indiscriminate mistranslation with Met protects cells from chloramphenicol (46), whereas Asp-to-Asn and Glu-to-Gln mistranslation endows *Mycobacteria* with increased resistance to rifampicin (47). The chemical diversity of these mistranslation events suggests that the randomization of the cellular protein pool may be more important than the identity of the misincorporated amino acid to decrease antibiotic susceptibility. Testing the effect of other forms of mistranslation on antibiotic resistance could provide more clues into this possibility and ultimately establish mistranslation as a bona fide mechanism of antibiotic resistance (57).

The biological function of the $tRNA^{ProX}$ family in their host organisms is yet to be investigated. However, the increased carbenicillin tolerance of *E. coli* cells expressing $tRNA^{ProN}$ suggests that Pro mistranslation may help $tRNA^{ProX}$-encoding organisms endure antibiotic exposure. It may also be possible that mistranslation offers an advantage in other environmental conditions, including in the adaptation of plant pathogenicity. However, ProRSx/$tRNA^{ProX}$ are not collocated with known plant virulence genes. Finally, despite the tRNAs' capacity to mistranslate the genetic code in *E. coli*, their biological function in the host species may lie outside protein synthesis. tRNAs are known to have diverse functions beyond translation (58). In some cases, a particular tRNA isoacceptor can be partitioned for non-ribosomal activities (59, 60). Thus, an alternative function of $tRNA^{ProX}$ regulated by cellular factors such as post-translational modifications or elongation factors is possible. Further investigations will define the biological role of $tRNA^{ProX}$ and establish the environmental conditions that promote their expression.

Experimental procedures

Identification of $tRNA^{ProA}$ and $tRNA^{ProA}$-like genes.

tRNA^{ProA} and tRNA^{ProA}-like genes were identified using the basic local alignment search tool (BLASTN) (61) hosted by the National Center for Biotechnology Information. The *Streptomyces turgidiscabies* tRNA^{ProA} sequence (STRTUCAR8_03649) was used as the query. Additional tRNA^{ProA} and tRNA^{ProA}-like genes were found using the "Compare Region Viewer" tool in the Bacterial and Viral Bioinformatics Resource Center (BR-BRC) (62, 63). The secondary structure and identity of the putative tRNA^{ProA} genes were predicted using tRNAscan-SE 2.0 (64). The manually aligned tRNA sequences are shown in Fig. S1.

Phylogenetic analysis and distribution of ProRSx and tRNA^{ProX}.

A total of 121 sequences corresponding to ProRSx (45), Bacterial-type ProRS (42), and Archaeal/Eukaryotic-type ProRS (34) were aligned using Clustal Omega (65). The Bacterial- and Archaeal/Eukaryotic-type ProRS sequences are from the organisms encoding ProRSx (Table S1). The sequence alignment was used to build the phylogenetic tree using MEGAX (66) with the Maximum Likelihood method with 100 bootstraps. The tree was visualized with iTOL (67). Multilocus sequence analysis alignments were generated with protein sequences of housekeeping genes from *Streptomyces scabiei* 87.22 (strepdb.streptomyces.org.uk) for atpD (SCO5373), gyrB (SCO3874), recA (SCO5769), rpoB (SCO4654), and trpB (SCO2037) against a local database of 84 genomes using automlsa2 (68, 69). The 46 genomes of strains that encode ProRSx or tRNA^{ProX} were complemented with 38 additional genomes selected to represent the diversity of *Streptomyces*, *Streptacidiphilus,* and *Kitasatospora* (39-41, 70). The *S. turgidiscabies* gene sequence (STRTUCAR8_03650) was used as the query against the local sequence database with a cutoff threshold of 1e-10 to confirm that ProRSx was not present in the other genomes. The ML tree was constructed using default parameters for iqtree2.2 and RAxML embedded in automlsa2 with 1000 bootstrap iterations. The R package ggtree was used to plot the phylogeny (71) and covariates.

Bacterial strains and plasmids.

E. coli Stellar™ cells (Takara) were used for cloning, and *E. coli* MG1655 was used for *in vivo* experiments. The HiFi DNA assembly kit (New England Biolabs) was used for molecular cloning. DNA sequencing was performed by Keck Biotechnology Resource Laboratory at Yale University to confirm plasmid sequences. The *Ks*ProRSx sequence was codon-optimized for expression in *E. coli* using the codon optimization tool from Integrated DNA Technologies. The corresponding DNA was purchased from Twist Bioscience. The *S. turgidiscabies* ProRSx (*St*ProRSx) gene was cloned into the pCDF vector. The *Ks*ProRSx was cloned into pCDF and pEVOL vectors (72). The tRNA^{ProA}, tRNA^{ProN}, and tRNA^{ProT} genes were cloned into either pCDF or pEVOL vectors under the *E. coli* constitutive promoter *proK*. A previously developed sfGFP-mCherry fusion reporter (31) was used to investigate *in vivo* mistranslation by tRNA^{ProT}. The ACC (Thr) codon at position 65 in sfGFP was mutated to ACU (Thr).

Growth conditions.

E. coli strains were grown in LB media at 37ºC and constant shaking. For selection, appropriate antibiotics carbenicillin (Cb, 100 µg/mL), spectinomycin (Spe, 100 µg/mL), kanamycin (Kan, 50 µg/mL), and chloramphenicol (Chl, 35 µg/mL) were supplemented to the media, unless otherwise indicated.

Growth assays.

Chemically competent *E. coli* MG1655 cells were transformed with the pCDF plasmid encoding a $tRNA^{ProX}$ gene with or without a *proSx* gene (*K. setae* or *S. turgidiscabies*). After transformation, cells were recovered in S.O.C. medium (Invitrogen) at 37ºC for 1 h with constant shaking. Following recovery, transformants were plated on LB-agar with respective antibiotics and grown overnight at 37ºC. Single colonies were used to inoculate 150 µL of fresh LB media with the corresponding antibiotics in black-sided 96-well plates with clear flat bottoms (Corning). Cell growth (optical density, OD) was measured at 600 nm (OD_{600}) for 20 h of incubation at 37ºC and constant shaking using a BioTek synergy HTX plate reader.

Fluorescence-based assays.

The pEVOL plasmid encoding $tRNA^{ProT}$ and the sfGFP-mCherry reporter plasmid were transformed into *E. coli* MG1655 cells. Single colonies were used to inoculate LB media containing Kan, Chl, and 0.2 mM IPTG to induce the expression of sfGFP-mCherry in a 96-well microplate. Cells were incubated for 24 h with constant shaking at 37ºC using a BioTek HTX plate reader. sfGFP (Excitation 485 nm, Emission 510 nm) and mCherry (Excitation 587 nm, Emission 610 nm) fluorescence and OD_{600} were measured. For consistency, we chose the individual mid-exponential growth phase of *E. coli* for determining sfGFP-mCherry fluorescence and mistranslation frequency. This was accomplished by determining the time at which *E. coli* cells reached the mid-exponential growth phase using the pre-set function "Sigmoidal, 4P, X is concentration" in Prism 9 (GraphPad). The sfGFP and mCherry fluorescence proportion was calculated at the mid-exponential growth phase.

β-Lactamase-based assays.

The mistranslation capacity of $tRNA^{ProN}$ was tested using a previously designed β-lactamase reporter (a gift from Dr. Ahmed Badran, Scripps) (31). The essential Pro residue at position 65 of β-lactamase was mutated to the Asn AAU codon. The activity of the resulting mutant was tested in *E. coli* S6020 cells. Cultures were prepared by inoculating LB media containing Kan with single colonies and grown overnight at 37ºC. 99 µL of fresh LB media with Kan and 62.5 µg/mL ampicillin was mixed with 1 µL of overnight culture. OD_{600} was monitored for 10 h at 37ºC with constant shaking using a BioTek synergy plate reader. Wild-type (wt) β-lactamase was used as a control. To test $tRNA^{ProN}$, the pCDF plasmid harboring $tRNA^{ProN}$ was co-transformed with the β-lactamase (P65N or wt) reporter plasmid into *E. coli* MG1655 cells. After transformation, cells were recovered for 1 h in S.O.C. medium with shaking at 37ºC. Subsequently, cells were plated on a selective LB-agar medium and incubated overnight at 37ºC. Cell cultures were obtained by inoculating 5 mL LB medium with a single colony and incubating overnight with constant shaking at 37ºC. The overnight cultures were diluted to OD_{600} of 1, which corresponded to the 10^0 dilutions, and then serially diluted to 10^1, 10^2, 10^3, 10^4, and 10^5. 4 µL of diluted cells were spotted on LB-agar plates with varying concentrations of carbenicillin (0 µg/mL, 20 µg/mL, 30 µg/mL, 40 µg/mL, and 50 µg/mL). The plates were imaged after for 18-20 h of incubation at 37ºC.

GFP purification and mass spectrometry analysis.

The peptide sequence MSKGPGKVPGAGVPG**X**GVPGVGKGGGT (43) was fused to the N-terminus of sfGFP containing a C-terminal 6xHis-tag in pBAD using HiFi DNA assembly. Position **X** indicates the Asn AAU codon**.** The resulting sfGFP variant was co-transformed with pCDF with or without the $tRNA^{ProN}$ gene into *E. coli* MG1655. Single colonies were used to inoculate LB media containing the antibiotics Cb and Spe. Cells were grown overnight at

37ºC. The overnight culture was used to inoculate fresh LB media with the corresponding antibiotics, and cells were grown to an OD_{600} of 0.4 - 0.6. sfGFP expression was induced with 0.15% arabinose for 5 h. The suspension cultures were harvested and lysed with Bugbuster® (Merck Millipore) and roll-incubated at room temperature for 20 min in a buffer containing 50 mM Tris-HCl (pH 8.0), 300 mM NaCl, 10 mM Imidazole, and cOmplete™ EDTA-free protease inhibitor mixture tablets (Roche), and 1 µL Benzonase® (Sigma-Aldrich). Lysed cells were centrifuged at 17,000 x *g* for 45 min at 4ºC. The lysate was passed through a TALON® Metal Affinity Resin (Takara Bio), and the proteins were eluted with 300 mM imidazole. Subsequently, the buffer with was exchanged to 50 mM Tris-HCl (pH 8.0) and 100 mM NaCl using Amicon® Ultra-4 centrifugal filter units (10.000 k, Merck Millipore) following protein concentration using the same filter units.

Samples were reduced with DTT and alkylated with IAA before digestion with trypsin and LysC. LC-MS/MS analysis was performed on a Thermo Scientific Orbitrap Fusion Lumos Tribrid mass spectrometer (ThermoFisher, San Jose, CA), equipped with a nanospray ionization source in positive ion mode with a Thermo Fisher Ultimate 3000 RSLCnano HPLC System (ThermoFisher). Peptide mixtures were loaded into a PEPMAP100 C18 5uM trap column (ThermoFisher) at a constant flow of 30uL/min, holding at 60°C. Peptides were eluted at a rate of 0.25 µL/min and separated using a PepSep reprosil c18, 1.9 µm, 15 cm ID 75 µM analytical column (Bruker) throughout a 60-min gradient: 0-50 min; 4% - 32% acetonitrile + 0.1% formic acid, 50-55 min; 95% acetonitrile + 0.1% formic acid, and 55-60 min; 4% acetonitrile + 0.1% formic acid.

MS data were acquired using the data-dependent mode with a cycle time of 3 sec. MS1 scan was performed in orbitrap within a range of 400-1600 m/z, at resolution 120000, and auto-injection time with a standard AGC target. RF lens was set to 30%. Isolation for MS2 scans was performed in the quadrupole, with an isolation window of 0.7. MS2 scans were done in the linear ion trap at turbo scan rate, with an auto maximum injection time and a standard AGC target level. HCD was used for generating the MS2 spectrum as fixed normalized collision energy of 30%. MS2 spectra were acquired at a 15000 resolution. All LC-MS/MS was performed at Bioinformatics Solutions Inc. in Waterloo, Ontario, Canada.

MS Raw Files were processed using PEAKS XPro (v10.6, Bioinformatics Solutions Inc., Ontario, Canada). The data was searched against a custom database containing the sfGFP sequence in the *E. coli* K12 Uniprot-reviewed database. Precursor ion mass error tolerance was set to 10 ppm, and fragment ion mass error tolerance was set to 0.02 Da. Semi-specific cleavage with trypsin or chymotrypsin was selected with a maximum of 3 missed cleavages. A fixed modification of carbamidomethylation (+57.02 Da) on cysteine residues was specified. Variable modifications of deamidation (+0.98 Da) on asparagine and glutamine, as well as oxidation (+15.99 Da) on methionine, were specified. A maximum of two variable modifications per peptide was allowed. The peptide false discovery rate was set to 1% for the database search. Only confident mutations with an A-Score of 20 or higher and minimum mutation ion intensities of 1% were considered. To ensure the accuracy in identifying mutations, we applied a false discovery rate (FDR) filter of <1% for peptide identification and minimum fragment ion intensity of 1% for each mutation.

Radiolabeling of oligonucleotide probes.

A 50 µL reaction mix containing 5 µL of 10 µM DNA oligonucleotide probes, 2.5 µL T4-polynucleotide kinase buffer (New England Biolabs), 37.5 µL RNase-free water, 5 µL γ-^{32}P-ATP (PerkinElmer), and 2.5 µL T4-polynucleotide kinase (New England Biolabs) was

prepared and incubated for 30 min at 37ºC. Excess γ-^{32}P-ATP was removed with Sephadex G-25 spin columns (Cytiva). Radioactivity of the oligonucleotides was measured with a scintillation counter (Tri-Carb 3110 TR, PerkinElmer).

Northern blot analysis.

E. coli MG1655 cells expressing tRNA^{ProA}, tRNA^{ProN}, or tRNA^{ProT} from a pCDF plasmid were grown overnight to inoculate fresh 20 mL LB media with appropriate antibiotics. Cells were grown to an OD_{600} of 0.4 and harvested by centrifugation at 4,000 x *g* at 4ºC. The cell pellet was resuspended in 0.5 mL extraction buffer (0.3 M sodium acetate pH 4.5, 10 mM EDTA) and lysed with 0.5 mL acidic phenol (pH 4.5). Samples were vortexed for 10 s and incubated on ice for 3 min. This step was repeated five times. Samples were then centrifuged for 12 min at 12,000 x *g* at 4ºC. The aqueous phase containing total RNA was collected, and the sample was re-extracted with 0.25 mL extraction buffer. RNA in the aqueous supernatant was precipitated by adding 2.5xV absolute ice-cold ethanol and incubated at -80ºC for 1 h. Samples were centrifuged for 20 min at 17,000 x *g* and 4ºC. The supernatant was discarded, and the RNA pellet was washed with 1 mL of 70% ice-cold ethanol. Centrifugation was repeated for 12 min. The supernatant was discarded, and the RNA pellet was air-dried. "Deacylated tRNA" samples were resuspended in 30 µL 200 µM Tris-HCl pH 8.0 and incubated for 30 min at 37ºC, while the "acylated tRNA" samples were resuspended in 30 µL 10 mM sodium acetate pH 4.5. RNA concentrations were measured with a spectrophotometer (NanoDrop C 2000, Thermo Scientific). Total RNA from *E. coli* MG1655 was isolated as described above. 1 µg of total RNA (15 µg for samples containing tRNA^{ProT}) was mixed with 2x loading buffer (0.1 M sodium acetate pH 5.0, 8 M Urea, 0.05% bromophenol blue, and 0.05% xylene cyanole). The samples were separated on a 6.5 % PAGE/7 M Urea gel (Outer Plate 22.3 x 20 cm (Bio-Rad), Inner Plate 20.0 x 20.0 cm (Bio-Rad), Spacer 0.5 mm (Bio-Rad)) in 0.1 M sodium acetate pH 5.0 at 150 V for 30 min and then 250 V for 7 h at 4ºC with a PROTEAN II xi electrophoresis cell (Bio-Rad). After separation, the gel region between bromophenol blue and xylene cyanole was excised and transferred to a wet Nylon membrane (GE Healthcare) in 0.5x TBE using a Trans-Blot® SD cell (Bio-Rad) at constant 25 V for 32 min. The RNA was cross-linked to the membrane in a UVC 500 Crosslinker (Amersham) and then hybridized with ^{32}P-labeled DNA probes targeting tRNA^{ProA} (5′-CAGGCTCCTCGGCAACG-3′), tRNA^{ProN} (5′-CGGCTCCTCGGCAGCAA-3′), and tRNA^{ProT} (5′-CAGCTCCTTGGCAACAC-3′) overnight at 42ºC. The membrane was exposed against a phosphor screen for 30 min for tRNA^{ProA} and tRNA^{ProN} and overnight for tRNA^{ProT}. The screen was imaged using a phosphoimager (Typhoon™, Amersham).

tRNA *in vitro* transcription and labeling.

tRNAs for *in vitro* aminoacylation assays were transcribed *in vitro*. The DNA template for *in vitro* transcription was generated via PCR from a plasmid containing a T7 promotor. After the PCR, DNA fragments were purified with a NucleoSpin® kit (Macherey-Nagel). For *in vitro* transcription, a 1 mL reaction mix of 1x transcription buffer (0.1 M Tris-HCl pH 8.0, 0.1 M $MgCl_2$, 2.3 M spermidine, 10% Triton, 10 mg/mL BSA, 50 mM DTT), 4 mM ATP, 4 mM GTP, 4 mM CTP, 4 mM UTP, 10 µg DNA template, 20 mM $MgCl_2$, DTT 5 mM, 10 µL pyrophosphatase (Roche) and T7 RNA polymerase was incubated at 37ºC for 16 h. Subsequently, the reaction was mixed with a 0.05% bromophenol blue, 0.05% xylene cyanole solution, and 50% formamide and separated with a 12% PAGE/8 M urea gel at

120 V overnight. tRNA bands were visualized under UV light and excised from the gel. The tRNA was extracted from the gel by grinding the excised gel piece and adding 1:2 extraction buffer (0.5 M ammonium acetate and 1 mM EDTA, pH 8.0). The gel solution was incubated at 37ºC with constant shaking overnight. The gel debris was sedimented by centrifugation at 4,000 x *g* for 10 min at 4ºC. The supernatant was filtered and concentrated using an Amicon® ultra (Merck) 10K filter. To precipitate the tRNA, 1xV absolute ice-cold ethanol was added and incubated at -80ºC for 1 h. The tRNAs were precipitated by centrifugation at 13,000 x *g* for 30 min at 4ºC. The supernatant was discarded, and the tRNA pellet was washed with ice-cold 70% ethanol and centrifuged at 13,000 x *g* for 10 min at 4ºC. The supernatant was discarded, and the pellet was air-dried and resuspended in 150 µL DEPC water. Subsequently, the tRNAs were labeled in a 100 µL reaction containing 50 mM glycine pH 9.0, 10 mM $MgCl_2$, 1 µM tRNA, 0.82 µM α-^{32}P-ATP (PerkinElmer), 50 µM sodium pyrophosphate, and 8.77 µg *E. coli* tRNA nucleotidyltransferase (73). The reaction was incubated for 5 min at 37ºC. 1 µL 100 µM CTP and 5 µL pyrophosphatase (Roche) were immediately added to the reaction mixture and incubated for another 2 min at 37ºC. The reaction was placed on ice, and the tRNA was extracted with 1xV acidic phenol pH 4.6 and centrifuged at 13,000 x *g* for 2 min at 4ºC. The aqueous phase was collected and re-extracted with acidic phenol. Excess α-^{32}P-ATP was removed with Sephadex G-25 spin columns (Cytiva). tRNA was precipitated by adding 2xV absolute ice-cold ethanol and 0.1xV ammonium acetate and incubated at -20ºC overnight. The tRNA solution was centrifuged at 13,000 x *g* for 45 min at 4ºC, and the supernatant was discarded. Subsequently, the tRNA pellet was washed with 300 µL 70% ice-cold ethanol and centrifuged at 13,000 x *g* for 10 min at 4ºC. The supernatant was discarded, and the ^{32}P-tRNA was resuspended in 30 µL of RNase-free water.

***In vitro* aminoacylation assays.**

Aminoacylation of $tRNA^{ProA}$, $tRNA^{ProN}$, $tRNA^{ProT}$, and *E. coli* $tRNA^{Pro}$ by *E. coli* ProRS was carried out in 50 mM HEPES pH 7.3, 8 mM ATP, 50 mM $MgCl_2$, 0.2 mg/mL BSA, 40 mM KCl, 40 mM β-mercaptoethanol, 1 mM proline, 7 µM tRNA, 3 µL γ-^{32}P-tRNA, and 1 µM ProRS in a final volume of 15 µL. Reactions were incubated at 37ºC and quenched at the indicated time points by mixing 1 µL of the reaction mix with 5 µL quenching solution (200 mM sodium acetate pH 5.0 and 0.1 U/µL nuclease P1 (Sigma Aldrich)). The quenched solutions were incubated for 1 h at room temperature. 1 µL was spotted on a cellulose matrix thin layer chromatography plate (Merck), pre-washed with water. The chromatography plate was run in a buffer containing 0.1 M sodium acetate pH 5.0, and 0.5% glacial acetic acid at room temperature. The plate was air-dried and exposed to a phosphor screen overnight. The screen was scanned using a phosphoimager, and the AMP and Pro-AMP spots were quantified using ImageJ 1.53 (NIH).

Statistical analysis

All assays were conducted independently, and the number of biological and technical replicates is specified in the figure legends. Statistical analyses were carried out using GraphPad Prism version 9.0 (GraphPad Software), with a two-tailed *t*-test used to assess statistical significance. A *p*-value of ≤0.05 was considered statistically significant. The results are presented as the mean ± standard deviation (SD). SDs are indicated as error bars.

Data availability

The mass spectrometry data have been deposited to the ProteomeXchange Consortium via the PRIDE (74) partner repository with the dataset identifier PXD041335 and 10.6019/PXD041335. All the other data is contained in the article. Requests for plasmids and other materials should be sent to: oscar.vargas@yale.edu.

Acknowledgments
Jonmatthew Bile was, in part, supported by an educational gift from Dr. Cecil B. Pickett. We thank Dr. Natalie Krahn for enlightening discussions and technical support, and Drs. Noah Reynolds and Jeffery Tharp for critically reading the manuscript. This work was supported by grants from the National Science Foundation (IOS-2151063 to O.V-R.) and the National Institute of General Medical Sciences (R35GM122560-05S1 to D.S.).

Conflict of interest
The authors declare no conflict of interest.

Author contributions
D.S., and O.V.-R. conceptualization; D.B.S., K.S.H., C.R.C., and O.V.-R. methodology; D.B.S., K.S.H., and O.V.-R. validation; D.B.S., and O.V.-R. formal analysis; D.B.S., J.T.F., J.B., S.A.G., B.A.S., A.A., and O.V.-R. investigation; M.J., D.S., C.R.C., and O.V.-R. resources; D.B.S., J.T.F., S.A.G., and O.V.-R. data curation; D.B.S., and O.V.-R. writing – original draft; D.B.S., J.T.F., B.A.S., M.J., K.S.H., E.W., D.S., C.R.C., and O.V.-R. writing – review and editing; D.B.S., B.A.S., K.S.H., E.W., and O.V.-R. visualization; D.S., and O.V.-R. supervision; D.S., and O.V.-R. project administration; D.S., and O.V.-R. funding acquisition.

References
1. Ribas de Pouplana, L., Santos, M. A. S., Zhu, J.-H., Farabaugh, P. J., and Javid, B. (2014) Protein mistranslation: friend or foe? *Trends Biochem. Sci.* **39**, 355-362
2. Kapur, M., and Ackerman, S. L. (2018) mRNA Translation Gone Awry: Translation Fidelity and Neurological Disease. *Trends Genet.* **34**, 218-231
3. Zhang, H., Lyu, Z., Fan, Y., Evans, C. R., Barber, K. W., Banerjee, K. *et al.* (2020) Metabolic stress promotes stop-codon readthrough and phenotypic heterogeneity. *Proc. Natl. Acad. Sci. U. S. A.* **117**, 22167-22172
4. Bullwinkle, T. J., Reynolds, N. M., Raina, M., Moghal, A., Matsa, E., Rajkovic, A. *et al.* (2014) Oxidation of cellular amino acid pools leads to cytotoxic mistranslation of the genetic code. *Elife* **3**,
5. Raina, M., Moghal, A., Kano, A., Jerums, M., Schnier, P. D., Luo, S. *et al.* (2014) Reduced amino acid specificity of mammalian tyrosyl-tRNA synthetase is associated with elevated mistranslation of Tyr codons. *J. Biol. Chem.* **289**, 17780-17790
6. Ling, J., and Söll, D. (2010) Severe oxidative stress induces protein mistranslation through impairment of an aminoacyl-tRNA synthetase editing site. *Proc. Natl. Acad. Sci. U. S. A.* **107**, 4028-4033
7. Brilkova, M., Nigri, M., Kumar, H. S., Moore, J., Mantovani, M., Keller, C. *et al.* (2022) Error-prone protein synthesis recapitulates early symptoms of Alzheimer disease in aging mice. *Cell Rep.* **40**, 111433
8. Shcherbakov, D., Nigri, M., Akbergenov, R., Brilkova, M., Mantovani, M., Petit, P. I. *et al.* (2022) Premature aging in mice with error-prone protein synthesis. *Sci. Adv.* **8**, eabl9051
9. Lant, J. T., Berg, M. D., Heinemann, I. U., Brandl, C. J., and O'Donoghue, P. (2019) Pathways to disease from natural variations in human cytoplasmic tRNAs. *J. Biol. Chem.* **294**, 5294-5308

10. Bacher, J. M., de Crécy-Lagard, V., and Schimmel, P. R. (2005) Inhibited cell growth and protein functional changes from an editing-defective tRNA synthetase. *Proc. Natl. Acad. Sci. U S A.* **102**, 1697-1701
11. Nangle, L. A., Motta, C. M., and Schimmel, P. (2006) Global effects of mistranslation from an editing defect in mammalian cells. *Chem. Biol.* **13**, 1091-1100
12. Lee, J. W., Beebe, K., Nangle, L. A., Jang, J., Longo-Guess, C. M., Cook, S. A. *et al.* (2006) Editing-defective tRNA synthetase causes protein misfolding and neurodegeneration. *Nature* **443**, 50-55
13. Pataskar, A., Champagne, J., Nagel, R., Kenski, J., Laos, M., Michaux, J. *et al.* (2022) Tryptophan depletion results in tryptophan-to-phenylalanine substitutants. *Nature* **603**, 721-727
14. Netzer, N., Goodenbour, J. M., David, A., Dittmar, K. A., Jones, R. B., Schneider, J. R. *et al.* (2009) Innate immune and chemically triggered oxidative stress modifies translational fidelity. *Nature* **462**, 522-526
15. Fan, Y., Wu, J., Ung, M. H., De Lay, N., Cheng, C., and Ling, J. (2015) Protein mistranslation protects bacteria against oxidative stress. *Nucleic Acids Res.* **43**, 1740-1748
16. Tuite, M. F., and Santos, M. A. S. (1996) Codon reassignment in Candida species: An evolutionary conundrum. *Biochimie* **78**, 993-999
17. Miranda, I., Rocha, R., Santos, M. C., Mateus, D. D., Moura, G. R., Carreto, L. *et al.* (2007) A Genetic Code Alteration Is a Phenotype Diversity Generator in the Human Pathogen *Candida albicans*. *PLoS One* **2**, e996
18. Suzuki, T., Ueda, T., and Watanabe, K. (1997) The 'polysemous' codon - a codon with multiple amino acid assignment caused by dual specificity of tRNA identity. *EMBO J.* **16**, 1122-1134
19. Rocha, R., Pereira, P. J. B., Santos, M. A. S., and Macedo-Ribeiro, S. (2011) Unveiling the structural basis for translational ambiguity tolerance in a human fungal pathogen. *Proc. Natl. Acad. Sci. U. S. A.* **108**, 14091-14096
20. Jones, T. E., Alexander, R. W., and Pan, T. (2011) Misacylation of specific nonmethionyl tRNAs by a bacterial methionyl-tRNA synthetase. *Proc. Natl. Acad. Sci. U. S. A.* **108**, 6933-6938
21. Mohler, K., and Ibba, M. (2017) Translational fidelity and mistranslation in the cellular response to stress. *Nat. Microbiol.* **2**, 17117
22. Samhita, L., Raval, P. K., and Agashe, D. (2020) Global mistranslation increases cell survival under stress in *Escherichia coli*. *PLoS Genet.* **16**, e1008654
23. Pan, T. (2013) Adaptive Translation as a Mechanism of Stress Response and Adaptation. *Annu. Rev. Genet.* **47**, 121-137
24. Kirchner, S., and Ignatova, Z. (2015) Emerging roles of tRNA in adaptive translation, signalling dynamics and disease. *Nat. Rev. Genet.* **16**, 98-112
25. Bacher, J. M., Waas, W. F., Metzgar, D., de Crécy-Lagard, V., and Schimmel, P. (2007) Genetic code ambiguity confers a selective advantage on *Acinetobacter baylyi*. *J. Bacteriol.* **189**, 6494-6496
26. Ling, J., O'Donoghue, P., and Söll, D. (2015) Genetic code flexibility in microorganisms: novel mechanisms and impact on physiology. *Nat. Rev. Microbiol.* **13**, 707-721
27. Hoffman, K. S., O'Donoghue, P., and Brandl, C. J. (2017) Mistranslation: from adaptations to applications. *Biochim. Biophys. Acta Gen. Subj.* **1861**, 3070-3080
28. Schwartz, M. H., and Pan, T. (2017) Function and origin of mistranslation in distinct cellular contexts. *Crit. Rev. Biochem. Mol. Biol.* **52**, 205-219
29. Lyu, Z., Wilson, C., and Ling, J. (2023) Translational Fidelity during Bacterial Stresses and Host Interactions. *Pathogens* **12**,
30. Garofalo, R., Wohlgemuth, I., Pearson, M., Lenz, C., Urlaub, H., and Rodnina, M. V. (2019) Broad range of missense error frequencies in cellular proteins. *Nucleic Acids Res.* **47**, 2932-2945
31. Vargas-Rodriguez, O., Badran, A. H., Hoffman, K. S., Chen, M., Crnkovi□, A., Ding, Y. *et al.* (2021) Bacterial translation machinery for deliberate mistranslation of the genetic code. *Proc. Natl. Acad. Sci. U. S. A.* **118**, e2110797118

32. Giegé, R., Sissler, M., and Florentz, C. (1998) Universal rules and idiosyncratic features in tRNA identity. *Nucleic Acids Res.* **26**, 5017-5035
33. Ibba, M., and Söll, D. (1999) Quality Control Mechanisms During Translation. *Science* **286**, 1893-1897
34. Guan, D., Grau, B. L., Clark, C. A., Taylor, C. M., Loria, R., and Pettis, G. S. (2012) Evidence that thaxtomin C is a pathogenicity determinant of Streptomyces ipomoeae, the causative agent of Streptomyces soil rot disease of sweet potato. *Mol. Plant. Microbe Interact.* **25**, 393-401
35. Bouchek-Mechiche, K., Gardan, L., Andrivon, D., and Normand, P. (2006) Streptomyces turgidiscabies and Streptomyces reticuliscabiei: one genomic species, two pathogenic groups. *Int J Syst Evol Microbiol.* **56**, 2771-2776
36. Nguyen, H. P., Shelley, B. A., Mowery, J., and Clarke, C. R. (2022) Description of Streptomyces griseiscabiei sp. nov. and reassignment of Streptomyces sp. strain NRRL B-16521 to Streptomyces acidiscabies. *Int. J. Syst. Evol. Microbiol.* **72**,
37. Nguyen, H. P., Weisberg, A. J., Chang, J. H., and Clarke, C. R. (2022) Streptomyces caniscabiei sp. nov., which causes potato common scab and is distributed across the world. *Int. J. Syst. Evol. Microbiol.* **72**,
38. Weisberg, A. J., Kramer, C. G., Kotha, R. R., Luthria, D. L., Chang, J. H., and Clarke, C. R. (2021) A Novel Species-Level Group of Streptomyces Exhibits Variation in Phytopathogenicity Despite Conservation of Virulence Loci. *Mol. Plant. Microbe Interact.* **34**, 39-48
39. Labeda, D. P., Dunlap, C. A., Rong, X., Huang, Y., Doroghazi, J. R., Ju, K. S. *et al.* (2017) Phylogenetic relationships in the family Streptomycetaceae using multi-locus sequence analysis. *Antonie Van Leeuwenhoek* **110**, 563-583
40. Li, Y., Wang, M., Sun, Z. Z., and Xie, B. B. (2021) Comparative Genomic Insights Into the Taxonomic Classification, Diversity, and Secondary Metabolic Potentials of Kitasatospora, a Genus Closely Related to Streptomyces. *Front Microbiol* **12**, 683814
41. Malik, A., Kim, Y. R., and Kim, S. B. (2020) Genome Mining of the Genus Streptacidiphilus for Biosynthetic and Biodegradation Potential. *Genes (Basel)* **11**,
42. Nakano, H., Okumura, R., Goto, C., and Yamane, T. (2002) *In vitro* combinatorial mutagenesis of the 65th and 222nd positions of the green fluorescent protein of *Aequarea victoria*. *Biotechnol. Bioprocess Eng.* **7**, 311-315
43. Mohler, K., Aerni, H. R., Gassaway, B., Ling, J., Ibba, M., and Rinehart, J. (2017) MS-READ: Quantitative measurement of amino acid incorporation. *Biochim. Biophys. Acta Gen. Subj.* **1861**, 3081-3088
44. McClain, W. H., Schneider, J., and Gabriel, K. (1994) Distinctive acceptor-end structure and other determinants of *Escherichia coli* $tRNA^{Pro}$ identity. *Nucleic Acids Res.* **22**, 522-529
45. Liu, H., Peterson, R., Kessler, J., and Musier-Forsyth, K. (1995) Molecular recognition of $tRNA^{Pro}$ by *Escherichia coli* proline tRNA synthetase *in vitro*. *Nucleic Acids Res.* **23**, 165-169
46. Schwartz, M. H., Waldbauer, J. R., Zhang, L., and Pan, T. (2016) Global tRNA misacylation induced by anaerobiosis and antibiotic exposure broadly increases stress resistance in *Escherichia coli*. *Nucleic Acids Res.* **44**, 10292-10303
47. Javid, B., Sorrentino, F., Toosky, M., Zheng, W., Pinkham, J. T., Jain, N. *et al.* (2014) Mycobacterial mistranslation is necessary and sufficient for rifampicin phenotypic resistance. *Proc. Natl. Acad. Sci. U. S. A.* **111**, 1132-1137
48. Mukai, T., Vargas-Rodriguez, O., Englert, M., Tripp, H. J., Ivanova, N. N., Rubin, E. M. *et al.* (2017) Transfer RNAs with novel cloverleaf structures. *Nucleic Acids Res.* **45**, 2776-2785
49. Sun, L., Gomes, A. C., He, W., Zhou, H., Wang, X., Pan, D. W. *et al.* (2016) Evolutionary Gain of Alanine Mischarging to Noncognate tRNAs with a G4:U69 Base Pair. *J. Am. Chem. Soc.* **138**, 12948-12955
50. Lant, J. T., Kiri, R., Duennwald, M. L., and O'Donoghue, P. (2021) Formation and persistence of polyglutamine aggregates in mistranslating cells. *Nucleic Acids Res.* **49**, 11883-11899

51. Berg, M. D., Giguere, D. J., Dron, J. S., Lant, J. T., Genereaux, J., Liao, C. *et al.* (2019) Targeted sequencing reveals expanded genetic diversity of human transfer RNAs. *RNA Biol.* **16**, 1574-1585
52. Hasan, F., Lant, J. T., and O'Donoghue, P. (2023) Perseverance of protein homeostasis despite mistranslation of glycine codons with alanine. *Philos. Trans. R. Soc. Lond. B Biol. Sci.* **378**, 20220029
53. MacArthur, M. W., and Thornton, J. M. (1991) Influence of proline residues on protein conformation. *J. Mol. Biol.* **218**, 397-412
54. Chan, P. P., and Lowe, T. M. (2016) GtRNAdb 2.0: an expanded database of transfer RNA genes identified in complete and draft genomes. *Nucleic Acids Res.* **44**, D184-189
55. Ruan, B., Palioura, S., Sabina, J., Marvin-Guy, L., Kochhar, S., Larossa, R. A. *et al.* (2008) Quality control despite mistranslation caused by an ambiguous genetic code. *Proc. Natl. Acad. Sci. U. S. A.* **105**, 16502-16507
56. Cozma, E., Rao, M., Dusick, M., Genereaux, J., Rodriguez-Mias, R. A., Villén, J. *et al.* (2022) Probing the genetic code and impacts of mistranslation using $tRNA^{Ala}$ anticodon variants. *bioRxiv* 2022.2011.2023.517754
57. Witzky, A., Tollerson, R., 2nd, and Ibba, M. (2019) Translational control of antibiotic resistance. *Open Biol.* **9**, 190051
58. Katz, A., Elgamal, S., Rajkovic, A., and Ibba, M. (2016) Non-canonical roles of tRNAs and tRNA mimics in bacterial cell biology. *Mol. Microbiol* **101**, 545-558
59. Giannouli, S., Kyritsis, A., Malissovas, N., Becker, H. D., and Stathopoulos, C. (2009) On the role of an unusual tRNAGly isoacceptor in Staphylococcus aureus. *Biochimie* **91**, 344-351
60. Rietmeyer, L., Fix-Boulier, N., Le Fournis, C., Iannazzo, L., Kitoun, C., Patin, D. *et al.* (2021) Partition of tRNAGly isoacceptors between protein and cell-wall peptidoglycan synthesis in Staphylococcus aureus. *Nucleic Acids Res* **49**, 684-699
61. Altschul, S. F., Gish, W., Miller, W., Myers, E. W., and Lipman, D. J. (1990) Basic local alignment search tool. *J. Mol. Biol.* **215**, 403-410
62. Olson, R. D., Assaf, R., Brettin, T., Conrad, N., Cucinell, C., Davis, J. J. *et al.* (2023) Introducing the Bacterial and Viral Bioinformatics Resource Center (BV-BRC): a resource combining PATRIC, IRD and ViPR. *Nucleic Acids Res.* **51**, D678-D689
63. Wattam, A. R., Davis, J. J., Assaf, R., Boisvert, S., Brettin, T., Bun, C. *et al.* (2017) Improvements to PATRIC, the all-bacterial Bioinformatics Database and Analysis Resource Center. *Nucleic Acids Res.* **45**, D535-D542
64. Chan, P. P., Lin, B. Y., Mak, A. J., and Lowe, T. M. (2021) tRNAscan-SE 2.0: improved detection and functional classification of transfer RNA genes. *Nucleic Acids Res.* **49**, 9077-9096
65. Sievers, F., Wilm, A., Dineen, D., Gibson, T. J., Karplus, K., Li, W. *et al.* (2011) Fast, scalable generation of high-quality protein multiple sequence alignments using Clustal Omega. *Mol. Syst. Biol.* **7**, 539
66. Stecher, G., Tamura, K., and Kumar, S. (2020) Molecular Evolutionary Genetics Analysis (MEGA) for macOS. *Mol. Biol. Evol.* **37**, 1237-1239
67. Letunic, I., and Bork, P. (2021) Interactive Tree Of Life (iTOL) v5: an online tool for phylogenetic tree display and annotation. *Nucleic Acids Res.* **49**, W293-W296
68. Davis, E. W., 2nd, Okrent, R. A., Manning, V. A., and Trippe, K. M. (2021) Unexpected distribution of the 4-formylaminooxyvinylglycine (FVG) biosynthetic pathway in Pseudomonas and beyond. *PLoS One* **16**, e0247348
69. Davis Ii, E. W., Weisberg, A. J., Tabima, J. F., Grunwald, N. J., and Chang, J. H. (2016) Gall-ID: tools for genotyping gall-causing phytopathogenic bacteria. *PeerJ* **4**, e2222
70. Labeda, D. P. (2016) Taxonomic evaluation of putative Streptomyces scabiei strains held in the ARS Culture Collection (NRRL) using multi-locus sequence analysis. *Antonie Van Leeuwenhoek* **109**, 349-356
71. Yu, G., Smith, D. K., Zhu, H., Guan, Y., and Lam, T. T.-Y. (2017) ggtree: an r package for visualization and annotation of phylogenetic trees with their covariates and other associated data. *Methods in Ecology and Evolution* **8**, 28-36

72. Young, T. S., Ahmad, I., Yin, J. A., and Schultz, P. G. (2010) An enhanced system for unnatural amino acid mutagenesis in *E. coli*. *J. Mol. Biol.* **395**, 361-374
73. Ledoux, S., and Uhlenbeck, O. C. (2008) [3'-32P]-labeling tRNA with nucleotidyltransferase for assaying aminoacylation and peptide bond formation. *Methods* **44**, 74-80
74. Perez-Riverol, Y., Bai, J., Bandla, C., Garcia-Seisdedos, D., Hewapathirana, S., Kamatchinathan, S. *et al.* (2022) The PRIDE database resources in 2022: a hub for mass spectrometry-based proteomics evidences. *Nucleic Acids Res.* **50**, D543-D552

Figure legends

Figure 1. The predicted cloverleaf structures of the $tRNA^{ProX}$ family. The three members of this family share the proline identity element, C1:G72 (indicated in red), but contain different anticodons. $tRNA^{ProA}$ contains the AGC alanine anticodon (shown in blue), while the newly discovered $tRNA^{ProT}$ and $tRNA^{ProN}$ have AGU threonine and AUU asparagine anticodons, respectively. Members of the $tRNA^{ProX}$ family have a combination of elements rarely found in canonical tRNAs (see Fig. S1), including G21, A33, A34, and the A15:A48 tertiary pair, which are indicated with orange asterisks in $tRNA^{ProA}$. The predicted secondary structures of canonical $tRNA^{Ala}$, $tRNA^{Asn}$, and $tRNA^{Thr}$ are shown with their predicted identity elements indicated in colored and bolded fonts (32). The tRNA sequences are from *Streptomyces turgidiscabies* ($tRNA^{Ala}$ and $tRNA^{ProA}$), *Streptomyces* sp. OK228 ($tRNA^{ProN}$ and $tRNA^{Asn}$), and *Kitasatospora setae* KM-6054 ($tRNA^{ProT}$ and $tRNA^{Thr}$).

Figure 2. The $tRNA^{ProX}$ operon. (A) The predicted operon organization of the $tRNA^{ProA}$, $tRNA^{ProT}$, and $tRNA^{ProN}$ families. All families are encoded upstream of a putative *murG* gene. $tRNA^{ProA}$ and some $tRNA^{ProT}$ genes are encoded downstream of a full-length *proSx* (ProRSx) gene (green), *GT4* (grey), *WbqC* (blue), and *lmbE* (brown). In some organisms, $tRNA^{ProT}$ is encoded in an operon composed of either only $tRNA^{ProT}$ and *murG* or a truncated *proSx* gene with a flanking methionine tRNA gene (*$tRNA^{Met}$*, orange). $tRNA^{ProN}$ is only found in operons with the *$tRNA^{Met}$* and truncated *proSx* configuration. The complete list of operons from each organism is shown in Figure S2. (B) Phylogeny of bacterial-encoded ProRS enzymes. The *branches* corresponding to the Bacterial-type and Archaeal/Eukaryotic-type ProRS isoforms (canonical isoforms in bacteria) are shown in the purple and light blue clusters, respectively. ProRSx sequences form a distinct cluster from the canonical ProRS enzymes. The $tRNA^{ProA}$-associated ProRSx sequences (green) diverge from the ProRSx encoded with $tRNA^{ProT}$ or $tRNA^{ProN}$ (red). Branches with bootstrap support higher than 80% are indicated by black triangles.

Figure 3. Phylogenetic distribution of ProRSx and $tRNA^{ProX}$. Maximum Likelihood phylogenetic tree constructed using multilocus sequence analysis from protein sequences of *Streptomyces* housekeeping genes *atpD*, *gyrB*, *recA*, *rpoB*, and *trpB*. Legend indicates the presence of ProRSx (brown, inner ring), pathogenicity (black, middle ring), and anticodon sequence for the corresponding $tRNA^{ProX}$ (outer ring). The scale bar represents the phylogenetic distance of 0.03 nucleotide substitutions per site. Strains NRRL S-984 and NRRL F-6133 were renamed from *Streptomyces* to *Kitasatospora* based on this MLSA.

Figure 4. Detection of Thr-to-Pro mistranslation by $tRNA^{ProT}$. (A) Schematic representation of the sfGFP/mCherry fusion reporter used for monitoring *in vivo* mistranslation of Thr (ACU) codons with Pro. T65 in sfGFP is essential for fluorophore formation and fluorescence (green circle), whereas Pro at this position impairs sfGFP fluorescence resulting in non-fluorescent protein (white circle). In cells expressing $tRNA^{ProT}$, Thr65 can be ambiguously translated as Thr and Pro, reducing the sfGFP fluorescence relative to cells without $tRNA^{ProT}$. mCherry fluorescence is used to normalize the expression of sfGFP. (B) *E. coli* MG1655 was transformed with plasmids encoding the sfGFP/mCherry reporter and $tRNA^{ProT}$ (with or without ProRSx), respectively. (C) The ratio of sfGFP and mCherry fluorescence at mid-exponential growth was measured in the presence of $tRNA^{ProT}$ only (green bar), ProRSx

only (brown bar), or both (orange bar). Bars represent the average of four biological replicates with the SD indicated. ns, not significant; **** $P<0.0001$ by *t* test.

Figure 5. *In vivo* translation activity of $tRNA^{ProN}$. (A) An N65 β-lactamase mutant is inactive and does not protect *E. coli* from β-lactam antibiotics. Cell growth (OD_{600}) was monitored for *E. coli* expressing wt (P65) or N65 β-lactamase in LB media containing ampicillin (62.5 μg/mL). Each time point is the average of three biological replicates with the SD indicated by the error bars. (B) Schematic representation of the β-lactamase reporter designed to monitor the translation of Asn AAU codons by $tRNA^{ProN}$ based on the critical functional role of the P65 residue. Mistranslation of Asn AAU at position 65 with Pro by $tRNA^{ProN}$ produces a mixed population of P65 and N65 β-lactamase, which can afford antibiotic resistance to cells. (C) Serial dilutions of *E. coli* cultures expressing either wt β-lactamase (wt β-Lac) or N65 β-lactamase (65N β-Lac) in the presence or absence of $tRNA^{ProN}$ were spotted on LB-agar plates containing 0 μg/mL, 30 μg/mL, and 50 μg/mL carbenicillin (Cb).

Figure 6. Toxicity of $tRNA^{ProX}$ genes in *E. coli*. $tRNA^{ProA}$, $tRNA^{ProN}$, and $tRNA^{ProT}$ were constitutively expressed in *E. coli* MG1655 cells in the presence and absence of cognate ProRSx. *Ks*ProRSx was co-expressed with $tRNA^{ProN}$ because $tRNA^{ProN}$ is found with a truncated ProRSx gene. Cell growth (OD_{600}) was monitored for 12 h (A) or measured after 20 h (B). The plotted results represent the average of four biological replicates with the corresponding SD indicated by the error bars. ns, not significant; * $P< 0.05$; **** $P< 0.0001$ by *t* test. (C) The density of overnight *E. coli* cultures expressing empty pCDF plasmid (control) or $tRNA^{ProX}$ genes alone is shown. Distinct colony sizes of *E. coli* cells were also observed on LB-agar plates (bottom panel).

Figure 7. Aminoacylation of $tRNA^{ProX}$ by *E. coli* ProRS. (A) *In vitro* aminoacylation of $tRNA^{ProA}$, $tRNA^{ProN}$, and $tRNA^{ProT}$ by *E. coli* ProRS. The reactions were carried out with 1 μM ProRS, 7 μM tRNA, and 1 mM proline at 37ºC for 30 min. Bars represent the average of three technical replicates with the SD indicated. Aminoacylation curves are shown in Figure S5 (B) Anticodon stem-loop representations of $tRNA^{Pro}$, $tRNA^{ProA}$, $tRNA^{ProN}$, and $tRNA^{ProT}$ are shown to highlight the difference in their anticodon sequence. Substitution of G36 to C or U in *E. coli* $tRNA^{Pro}$ is known to decrease aminoacylation efficiency by *E. coli* ProRS by 164- and 9-fold, respectively (45). (C) The steady-state aminoacylation levels of $tRNA^{ProX}$ expressed in *E. coli* were determined by Northern blotting. Total RNA was extracted from cells expressing plasmid-borne $tRNA^{ProN}$, $tRNA^{ProA}$, or $tRNA^{ProT}$ under acidic conditions. A fraction of the sample was then treated with NaOH to remove the amino acids from tRNAs ("deacylated"). The RNA was separated in an acid-urea gel, and tRNAs were detected by hybridization with specific radiolabeled DNA probes.

Figure 8. Increased antibiotic tolerance of *E. coli* cells expressing $tRNA^{ProN}$ or $tRNA^{ProA}$. (A) *E. coli* MG1655 cells harboring the plasmid encoding wt β-lactamase were transformed with a plasmid containing the $tRNA^{ProN}$ or $tRNA^{ProA}$ gene. (B) Serial dilutions of overnight cultures were spotted on LB-agar plates containing 0 μg/mL, 100 μg/mL, and 250 μg/mL carbenicillin (Cb). The plates were incubated at 37ºC for 24 h.

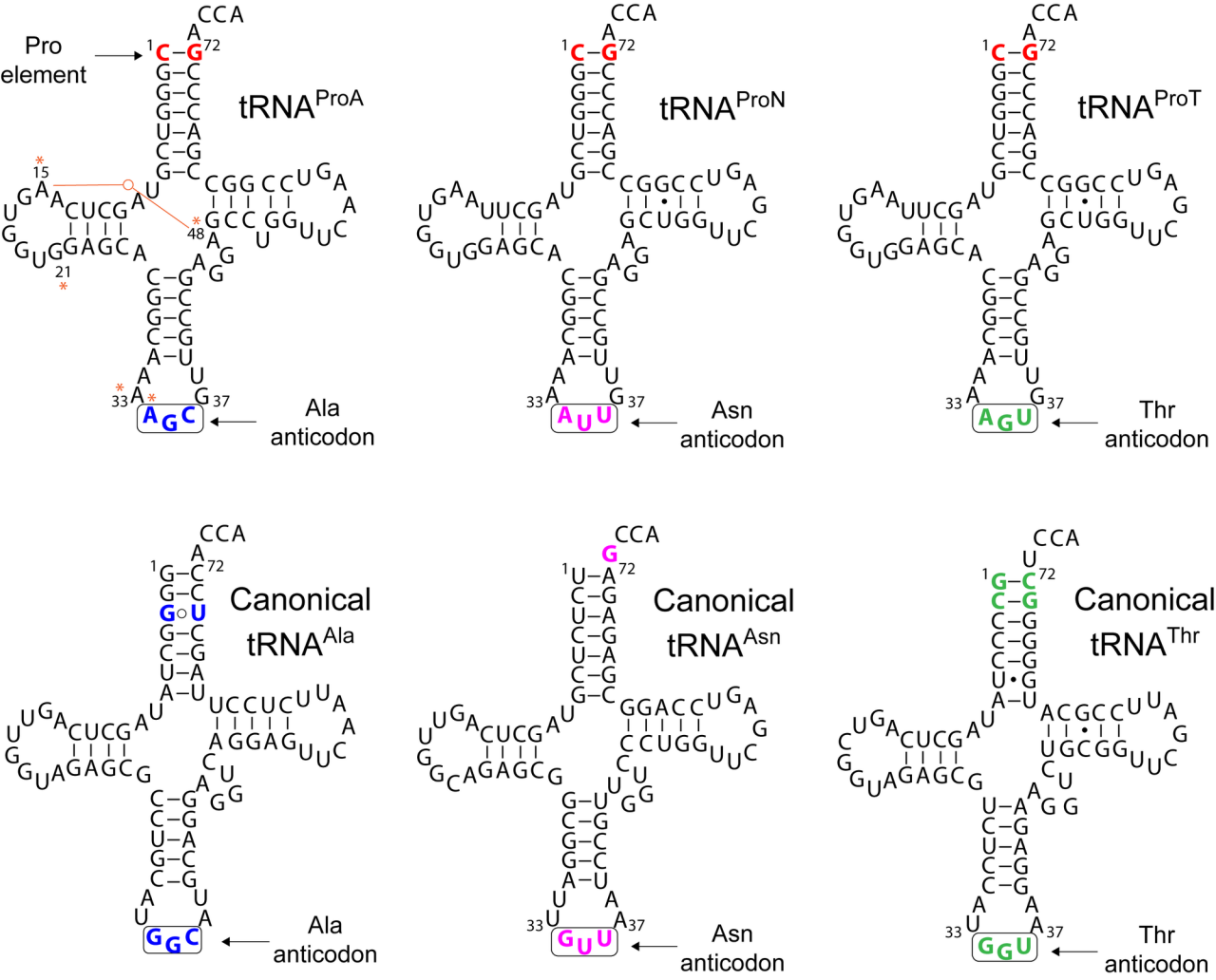
Pro element
tRNA^ProA
Ala anticodon
tRNA^ProN
Asn anticodon
tRNA^ProT
Thr anticodon
Canonical tRNA^Ala
Ala anticodon
Canonical tRNA^Asn
Asn anticodon
Canonical tRNA^Thr
Thr anticodon

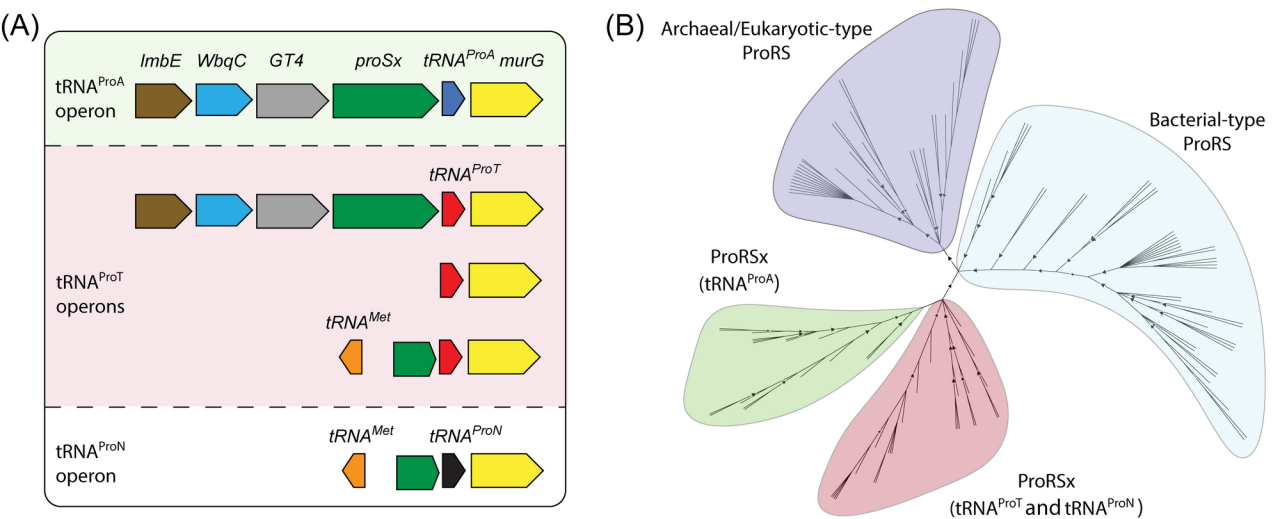
(A)
lmbE
WbqC
GT4
proSx
tRNA^ProA
murG
tRNA^ProA operon
tRNA^ProT
tRNA^ProT operons
tRNA^Met
tRNA^Met
tRNA^ProN
tRNA^ProN operon
(B)
Archaeal/Eukaryotic-type ProRS
Bacterial-type ProRS
ProRSx (tRNA^ProA)
ProRSx (tRNA^ProT and tRNA^ProN)

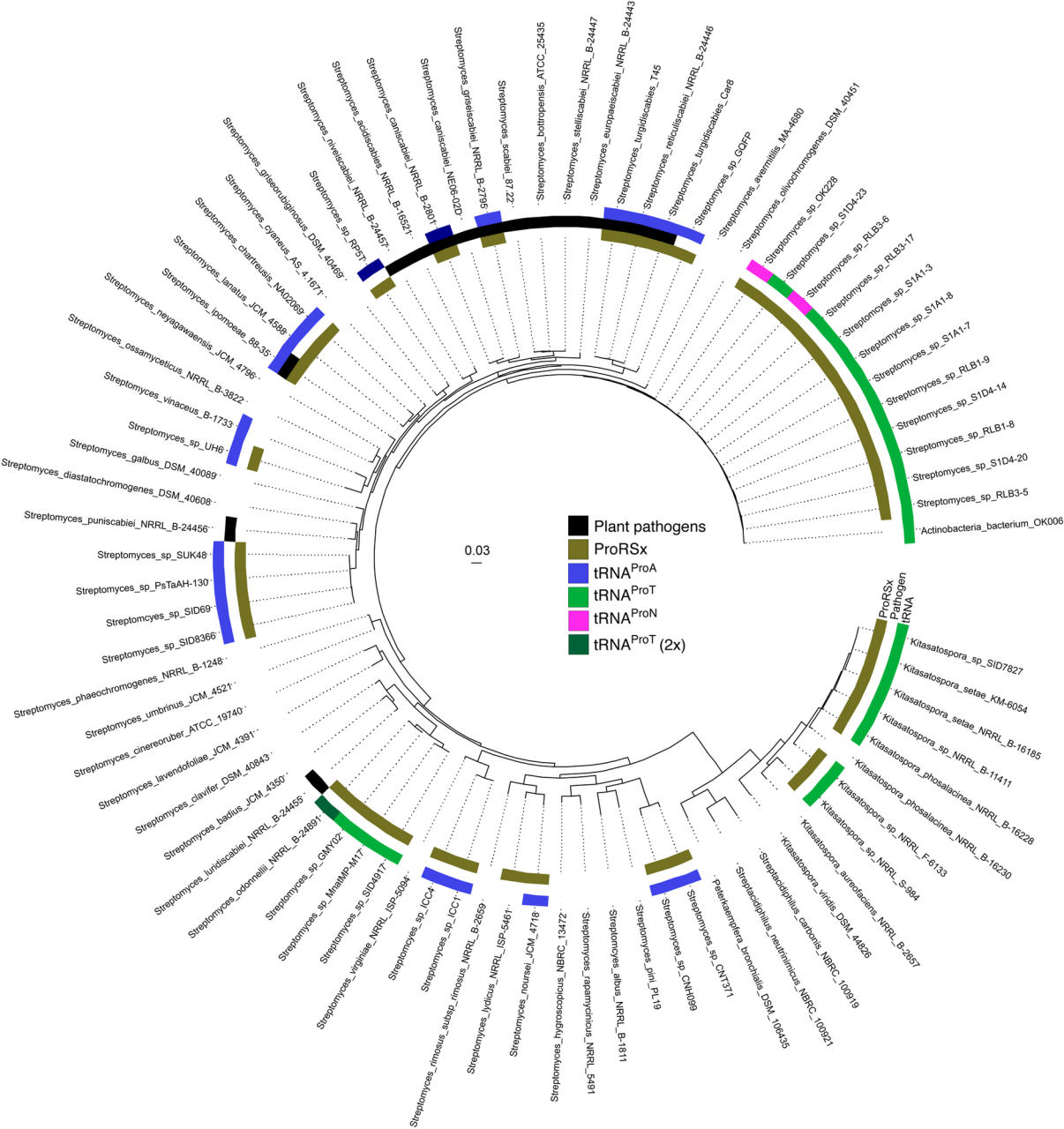
Streptomyces_griseiscabiei_NRRL_B-2795
Streptomyces_scabiei_87.22
Streptomyces_bottropensis_ATCC_25435
Streptomyces_stelliscabiei_NRRL_B-24447
Streptomyces_europaeiscabiei_NRRL_B-24443
Streptomyces_turgidiscabies_T45
Streptomyces_reticuliscabiei_NRRL_B-24446
Streptomyces_turgidiscabies_Car8
Streptomyces_sp_GQFP
Streptomyces_avermitilis_MA-4680
Streptomyces_olivochromogenes_DSM_40451
Streptomyces_sp_OK228
Streptomyces_sp_S1D4-23
Streptomyces_sp_RLB3-6
Streptomyces_sp_RLB3-17
Streptomyces_sp_S1A1-3
Streptomyces_sp_S1A1-8
Streptomyces_sp_S1A1-7
Streptomyces_sp_RLB1-9
Streptomyces_sp_S1D4-14
Streptomyces_sp_RLB1-8
Streptomyces_sp_S1D4-20
Streptomyces_sp_RLB3-5
Actinobacteria_bacterium_OK006
Streptomyces_griseorubiginosus_DSM_40469
Streptomyces_cyaneus_AS_4.1671
Streptomyces_chartreusis_NA02069
Streptomyces_lanatus_JCM_4588
Streptomyces_ipomoeae_88-35
Streptomyces_neyagawaensis_JCM_4786
Streptomyces_ossamyceticus_NRRL_B-3822
Streptomyces_vinaceus_B-1733
Streptomyces_sp_UH6
Streptomyces_galbus_DSM_40089
Streptomyces_diastatochromogenes_DSM_40608
Streptomyces_puniscabiei_NRRL_B-24456
Streptomyces_sp_SUK48
Streptomyces_sp_PsTaAH-130
Streptomyces_sp_SID69
Streptomyces_sp_SID8366
Streptomyces_nivealiscabiei_NRRL_B-24457
Streptomyces_sp_RP5T
Streptomyces_acidiscabies_NRRL_B-16521
Streptomyces_caniscabiei_NRRL_B-2801
Streptomyces_caniscabiei_NE06-02D
Streptomyces_phaeochromogenes_NRRL_B-1248
Streptomyces_umbrinus_JCM_4521
Streptomyces_cinereoruber_ATCC_19740
Streptomyces_lavendofoliae_JCM_4391
Streptomyces_clavifer_DSM_40843
Streptomyces_badius_JCM_4350
Streptomyces_lundiscabiei_NRRL_B-24455
Streptomyces_odonnelliii_NRRL_B-24691
Streptomyces_sp_GMY02
Streptomyces_sp_MnatMP-M17
Streptomyces_sp_SID4917
Streptomyces_virginiae_NRRL_ISP-5094
Streptomyces_sp_ICC4
Streptomyces_sp_ICC1
Streptomyces_rimosus_subsp_rimosus_NRRL_B-2659
Streptomyces_lydicus_NRRL_ISP-5461
Streptomyces_noursei_JCM_4718
Streptomyces_hygroscopicus_NBRC_13472
Streptomyces_rapamycinicus_NRRL_5491
Streptomyces_albus_NRRL_B-1811
Streptomyces_pini_PL19
Streptomyces_sp_CNH099
Streptomyces_sp_CNT371
Peterkaempfera_bronchialis_DSM_106435
Streptacidiphilus_neutrinimicus_NBRC_100921
Streptacidiphilus_carbonis_NBRC_100919
Kitasatospora_viridis_DSM_44826
Kitasatospora_aureofaciens_NRRL_B-2857
Kitasatospora_sp_NRRL_S-984
Kitasatospora_sp_NRRL_F-6133
Kitasatospora_phosalacinea_NRRL_B-16230
Kitasatospora_phosalacinea_NRRL_B-16228
Kitasatospora_sp_NRRL_B-11411
Kitasatospora_setae_NRRL_B-16185
Kitasatospora_setae_KM-6054
Kitasatospora_sp_SID7827
ProRSx
Pathogen
tRNA
Plant pathogens
ProRSx
tRNA^ProA
tRNA^ProT
tRNA^ProN
tRNA^ProT (2x)
0.03

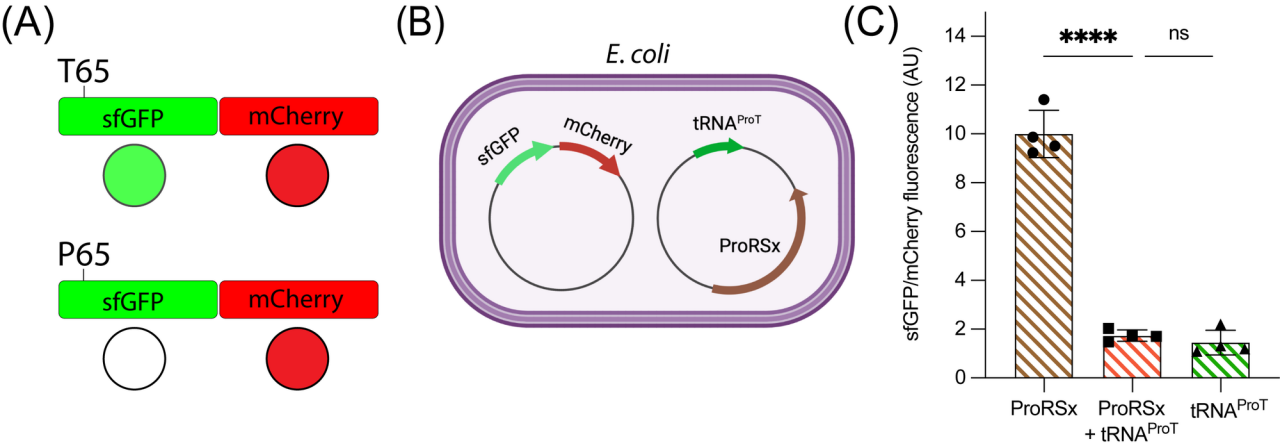
(A)
T65
sfGFP
mCherry
P65
sfGFP
mCherry
(B)
E. coli
sfGFP
mCherry
tRNAProT
ProRSx
(C)
sfGFP/mCherry fluorescence (AU)
0
2
4
6
8
10
12
14
****
ns
ProRSx
ProRSx + tRNAProT
tRNAProT

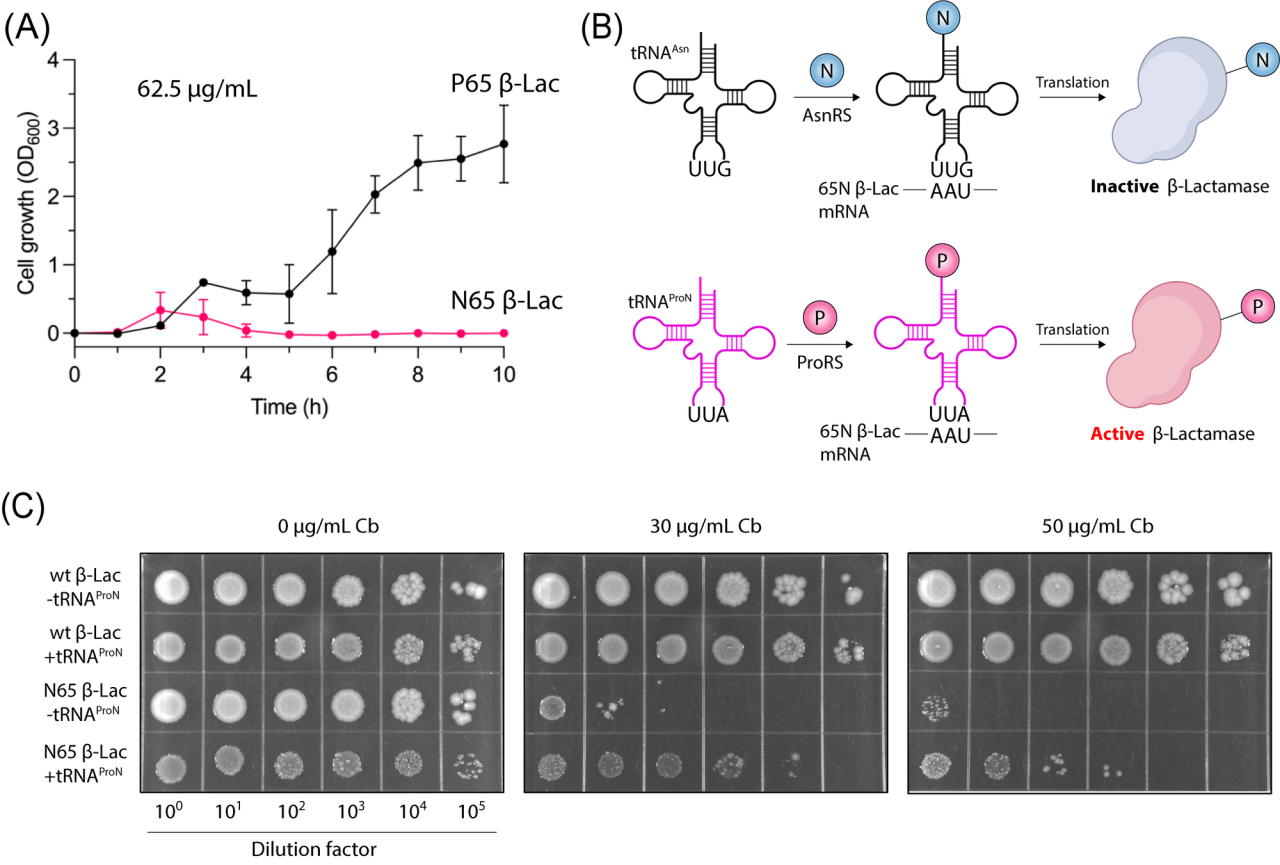
(A)
62.5 µg/mL
P65 β-Lac
N65 β-Lac
Cell growth (OD600)
Time (h)
(B)
tRNAAsn
UUG
N
AsnRS
65N β-Lac mRNA
AAU
Translation
Inactive β-Lactamase
tRNAProN
UUA
P
ProRS
Active β-Lactamase
(C)
0 µg/mL Cb
30 µg/mL Cb
50 µg/mL Cb
wt β-Lac -tRNAProN
wt β-Lac +tRNAProN
N65 β-Lac -tRNAProN
N65 β-Lac +tRNAProN
10^0 10^1 10^2 10^3 10^4 10^5
Dilution factor

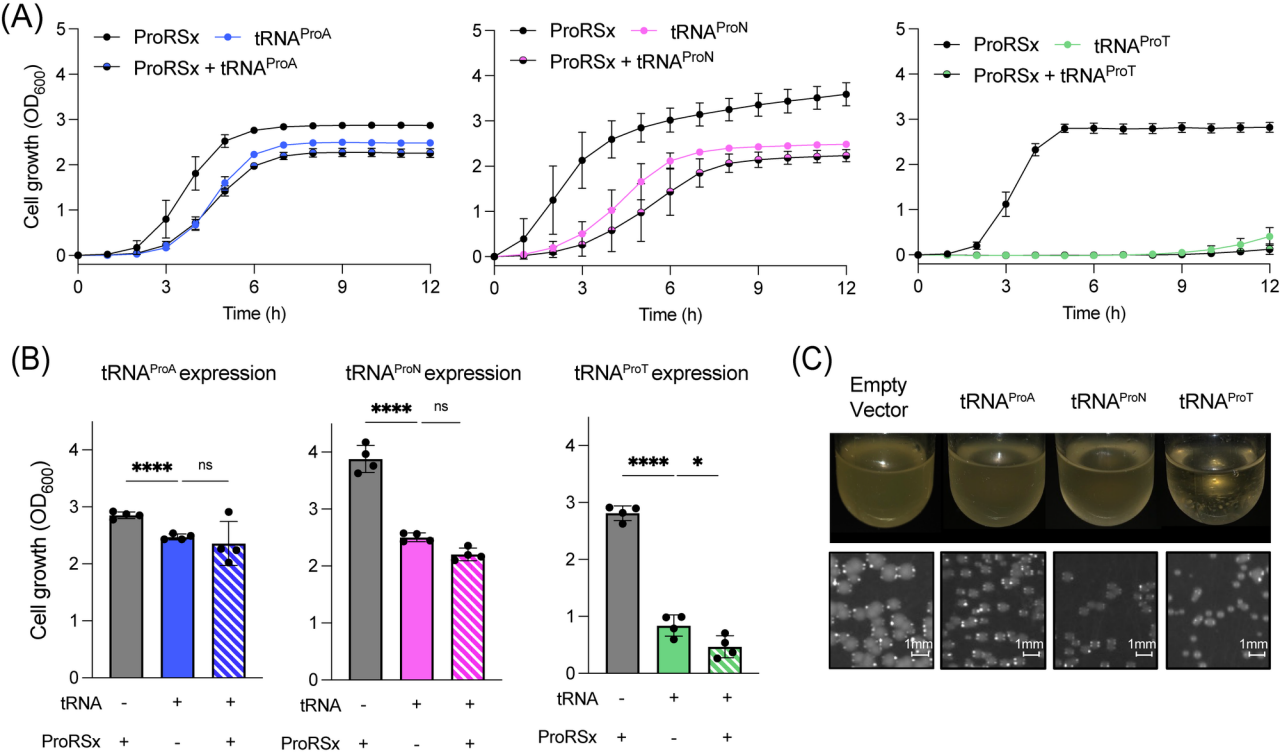
(A)
ProRSx
tRNA^ProA
ProRSx + tRNA^ProA
Cell growth (OD600)
Time (h)
ProRSx
tRNA^ProN
ProRSx + tRNA^ProN
Time (h)
ProRSx
tRNA^ProT
ProRSx + tRNA^ProT
Time (h)
(B)
tRNA^ProA expression
tRNA^ProN expression
tRNA^ProT expression
Cell growth (OD600)
****
ns
****
ns
****
*
tRNA - + +
ProRSx + - +
(C)
Empty Vector
tRNA^ProA
tRNA^ProN
tRNA^ProT
1mm

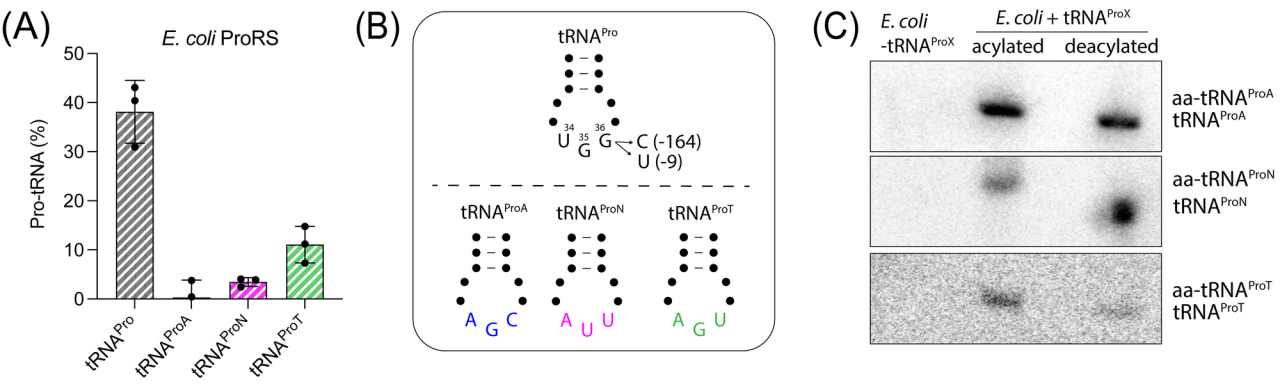
(A)
E. coli ProRS
Pro-tRNA (%)
50
40
30
20
10
0
tRNAPro
tRNAProA
tRNAProN
tRNAProT
(B)
tRNAPro
U 34 G 35 G 36
C (-164)
U (-9)
tRNAProA
tRNAProN
tRNAProT
A G C
A U U
A G U
(C)
E. coli -tRNAProX
E. coli + tRNAProX
acylated
deacylated
aa-tRNAProA
tRNAProA
aa-tRNAProN
tRNAProN
aa-tRNAProT
tRNAProT

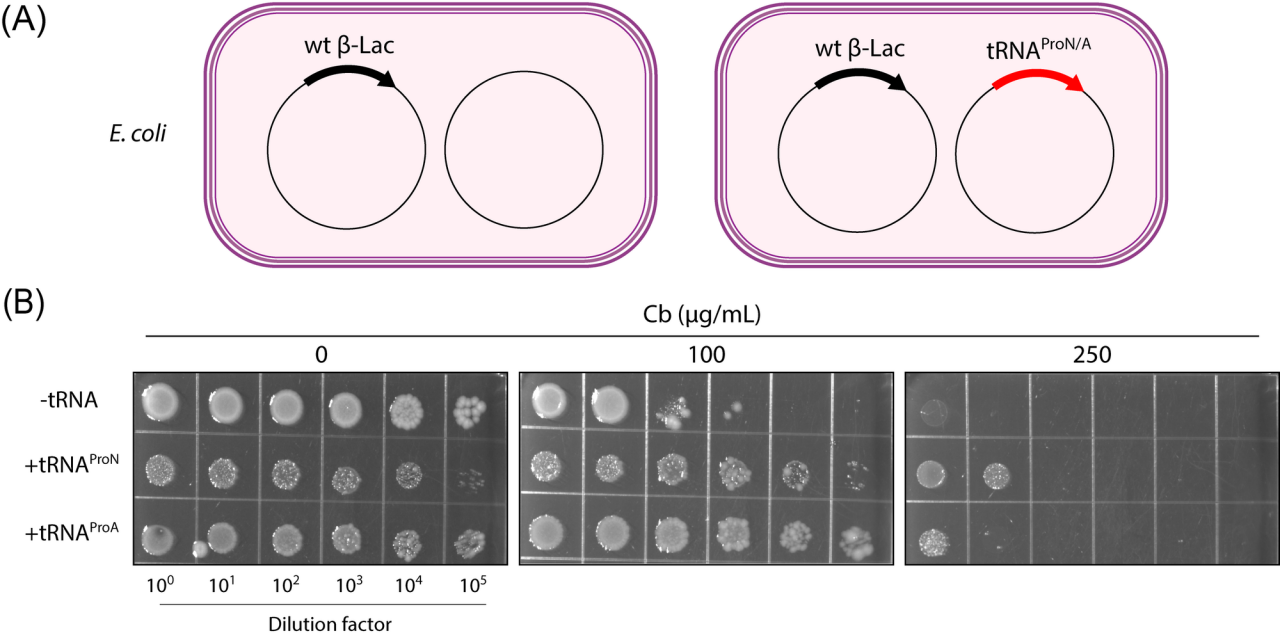
(A)
E. coli
wt β-Lac
wt β-Lac
tRNA ProN/A
(B)
Cb (µg/mL)
0
100
250
-tRNA
+tRNA ProN
+tRNA ProA
10 0
10 1
10 2
10 3
10 4
10 5
Dilution factor